Environment International 196 (2025) 109306

Contents lists available at ScienceDirect

Environment International

journal homepage: www.elsevier.com/locate/envint

Full length article

Metabolic and molecular Characterization, following dietary exposure to DINCH, Reveals new Implications for its role as a Metabolism-Disrupting chemical

Sontje Krupka [a,e,1], Alix Sarah Aldehoff [b,1], Cornelius Goerdeler [b,1], Beatrice Engelmann [b], Ulrike Rolle-Kampczyk [b], Kristin Schubert [b,*], Nora Klöting [a,*], Martin von Bergen [b,c,d,1,*], Matthias Blüher [a,e]

[a] Helmholtz Institute for Metabolic, Obesity and Vascular Research (HI-MAG) of the Helmholtz Centre München at the University of Leipzig Germany
[b] Department of Molecular Toxicology, Helmholtz-Centre for Environmental Research GmbH (UFZ) Leipzig Germany
[c] Institute of Biochemistry Faculty of Biosciences, Pharmacy and Psychology Leipzig University Leipzig Germany
[d] German Centre for Integrative Biodiversity Research (iDiv) Halle-Jena-Leipzig Leipzig Germany
[e] Department of Endocrinology Nephrology Rheumatology University Hospital Leipzig Medical Research Center Leipzig Germany

ARTICLE INFO

Keywords:
DINCH
MINCH
Metabolic disruption
Obesity
Adipose tissue

ABSTRACT

Plastic materials are ubiquitous, leading to constant human exposure to plastic additives such as plasticizers. There is growing evidence that plasticizers may contribute to obesity due to their disruptive effects on metabolism. Alternatives like diisononylcyclohexane-1,2-dicarboxylate (DINCH) are replacing traditional phthalates such as di-(2-ethylhexyl) phthalate (DEHP), which are now banned due to their proven harmful health effects. While DINCH is considered a safer alternative to DEHP and no adipogenic effects have been demonstrated in *in vivo* studies, recent research suggests that the primary metabolite, monoisononylcyclohexane-1,2-dicarboxylic acid ester (MINCH), promotes adipocyte differentiation and dysfunction *in vitro*. However, metabolic and molecular effects are not fully understood *in vivo*.

Here, we performed a comprehensive *in vivo* analysis using C57BL/6N mice to investigate the effects of DINCH on adipose tissue physiology and function. Mice were exposed to two doses of DINCH for 16 weeks, followed by a 10-week recovery period. Tissue analysis confirmed the presence of DINCH and MINCH in liver and adipose tissue after treatment and recovery. After the recovery period, elevated DINCH concentrations in adipose tissue depots indicated possible bioaccumulation. Although no changes were observed in body composition and energy expenditure, sex-specific metabolic effects were identified. Female mice exhibited impaired whole-body insulin sensitivity and higher triglyceride levels, while male mice showed an altered insulin/C-peptide ratio and elevated cholesterol, HDL, and LDL levels. Proteomic profiling of serum, adipose and liver tissues revealed changes in pathways related to central energy metabolism and immune response, highlighting the systemic impact of DINCH, potentially on inflammatory processes. Most effects of DINCH, such as changes in insulin response and serum lipid levels, were diminished after the recovery period.

Despite many findings consistent with the existing literature suggesting DINCH as a safer DEHP substitute, the observed sex-specific effects on insulin sensitivity, lipid metabolism and inflammatory processes, as well as potential bioaccumulation and long-term metabolic effects of DINCH exposure warrant careful consideration in further risk assessment.

1. Introduction

Over the past decades, the exponential growth in production and ubiquitous presence of plastic materials has prompted concerns about its potential impact on human health (Meeker et al., 2009; Wright & Kelly, 2017). This period has also witnessed a notable rise in the rates of people

* Corresponding authors.
E-mail addresses: kristin.schubert@ufz.de (K. Schubert), nora.kloeting@helmholtz-munich.de (N. Klöting), martin.vonbergen@ufz.de (M. von Bergen).
[1] Authors contributed equally.

https://doi.org/10.1016/j.envint.2025.109306
Received 29 August 2024; Received in revised form 20 December 2024; Accepted 24 January 2025
Available online 26 January 2025
0160-4120/© 2025 The Authors. Published by Elsevier Ltd. This is an open access article under the CC BY license (http://creativecommons.org/licenses/by/4.0/).

with overweight and obesity (NCD Risk Factor Collaboration, 2017). Plastic additives, specifically plasticizers, have been identified as a potential contributing factor to adipose tissue dysfunction, which may lead to obesity and associated metabolic disorders (Harley et al., 2017; Huang et al., 2014; Yaghjyan et al., 2015).

Plasticizers are essential components of plastic materials that improve their flexibility, pliability, and elasticity, particularly in PVC materials (Andrady & Neal, 2009). They are not covalently bound to the polymer matrix and can readily migrate into the surrounding environment (Hahladakis et al., 2018). Consequently, humans are exposed to plasticizers through various routes, including ingestion, dermal absorption, inhalation, and parenteral/intravenous exposure (Giovanoulis et al., 2018; Stevens et al., 2024).

Among the plasticizers, phthalates are the most commonly used group worldwide (Godwin, 2017). Several *in vivo* studies indicate that mono-2-ethylhexyl phthalate (MEHP), the primary metabolite of the prominent phthalate plasticizer di-2-ethylhexyl phthalate (DEHP), displays obesogenic properties (Biemann et al., 2021). These include the promotion of weight gain, the alteration of adipokine or lipid levels in serum (Hao et al., 2012; Klöting et al., 2015; Schmidt et al., 2012) and impairment of insulin tolerance in mice (Klöting et al., 2015). Due to their endocrine-disrupting properties, the use of DEHP and other phthalates has been prohibited in the European Union (EU) for specific applications since 1999 (European Commission (EC), 1999).

In the search for safer alternatives, non-phthalates such as diisononyl-cyclohexane-1,2-dicarboxylate (DINCH) emerged as a potential substitute for DEHP in plastic materials, particularly in everyday consumer products like toys, medical devices, and food packaging (Harmon & Otter, 2022; Kasper-Sonnenberg et al., 2019). Although DINCH displays structural similarity to phthalates, approval studies indicate more favorable toxicological properties (European Food Safety Authority (EFSA), 2006; Harmon & Otter, 2022). Still, it was shown that the primary metabolite of DINCH, monoisononyl-cyclohexane-1,2-dicarboxylic acid ester (MINCH), promotes adipocyte differentiation and increases lipid accumulation in the rat stromal vascular fraction (Campioli et al., 2017). Further studies in the human SGBS preadipocyte cell line have demonstrated that MINCH induces adipogenesis by altering the abundance of key enzymes and metabolites of the central carbon metabolism towards *de novo* lipogenesis (Goerdeler et al., 2024; Schaffert et al., 2022). The effects of MINCH are predominantly attributed to the activation of the nuclear receptor peroxisome proliferator-activated receptor gamma (PPARG) (Goerdeler et al., 2024; Schaffert et al., 2022; Useini et al., 2023), which is a central regulator of adipogenesis and adipocyte metabolism (Lefterova et al., 2014). Notably, the effects of MINCH on preadipocytes observed in the *in vitro* studies occurred primarily at micromolar concentrations (Campioli et al., 2017; Goerdeler et al., 2024; Schaffert et al., 2021), which exceed current exposure levels within the general population. However, effects on mature human SGBS adipocytes, such as changes in adipokine secretion and lipid metabolism, were already observed at low nanomolar concentrations (Schaffert et al., 2021), which are comparable to the concentrations of phthalate plasticizers found in human serum (Högberg et al., 2008; Specht et al., 2014).

In contrast to the *in vitro* studies, a comprehensive review of approval studies conducted in Wistar rats found no evidence of changes in body weight, altered lipid metabolism, or adipogenic properties associated with Hexamoll® DINCH exposure (Langsch et al., 2018). These *in vivo* studies were conducted according to *The Organization for Economic Cooperation and Development* (OECD) guidelines, which are currently not explicitly designed to identify potential metabolic disruptive properties and effects on adipose tissue depots (visceral, subcutaneous, brown) or adipokine secretion (e.g. leptin, adiponectin, monocyte chemoattractant protein-1 (MCP-1)) (Braeuning et al., 2023). This knowledge gap highlights the necessity for comprehensive *in vivo* studies to fully assess the physiological and functional consequences of DINCH exposure on adipose tissue, including effects at the molecular scale.

To investigate the metabolic and molecular effects of DINCH *in vivo*, a diet–induced obesity (DIO) mouse model of C57BL/6N mice was exposed to two doses of DINCH for 16 weeks, followed by a 10-week recovery period to assess a potential reversal of effects. Exposure was evaluated by determining the concentrations of DINCH, MINCH, and their secondary metabolites in liver and adipose tissue depots. Metabolic effects were characterized by analyzing body composition, whole-body insulin sensitivity, and energy expenditure. The molecular effects of DINCH were assessed through proteome profiling of liver and adipose tissue depots, as well as serum proteomics and metabolomics analyses. This study emphasizes the need to carefully incorporate molecular profiles and their alterations to gain a comprehensive understanding of the chemical modes of action that may play a role in metabolic diseases.

2. METHODS

2.1. Animal housing, handling and phenotypic characterization

All animal experiments were conducted in strict adherence to the guidelines approved by the local authorities of the State of Saxony, Germany, as recommended by the responsible animal ethics review board (Regierungspräsidium Leipzig, TVV38/20, Germany). C57BL/6N mice (RRID:IMSR_TAC:B6; Taconic Biosciences, USA) were bred and housed under pathogen-free conditions, with 3–4 mice per cage, in the SIKT – *Sächsischer Inkubator für Klinische Translation* (University of Leipzig, Leipzig). The mice were maintained at a controlled ambient temperature of 23 °C, with a 12-hour light/dark cycle. Throughout the study, all mice had unrestricted access to both water and food.

The experimental groups consisted of mice that were fed either (1) a standard chow diet (SD; V1534, 9 kJ% fat, Ssniff®, Germany) or (2) a high-fat diet (HFD; containing 59 kJ% from fat; E15772-34, Ssniff®, Germany) including two concentrations of 1,2-Cyclohexane dicarboxylic acid diisononyl ester (DINCH, IUPAC Bis(7-methyloctyl) cyclohexane-1,2-dicarboxylate, 95 %, CAS 166412–78-8, Article number AB440048, abcr GmbH, Germany). The DINCH concentrations used were (3) 4,500 ppm (LD) and (4) 15,000 ppm (HD) and were incorporated into the high-fat diet (HFD) by the feed provider, ssniff Spezialdiäten GmbH (Soest, Germany). These doses were selected to be comparable to the concentrations used in the metabolome study described by Langsch et al. 2018, in which Wistar rats received DINCH at a dietary concentration of 4,500 ppm and 15,000 ppm for 28 days. To prevent lipid degradation through oxidation, the HFD pellets were stored at −20 °C until use. The dietary intervention started at the age of four weeks and continued for 16 weeks. The diet was provided to the mice ad libitum, ensuring continuous availability throughout the exposure period. In the following, the mice were divided into two groups; one group underwent endpoint analysis (Treatment), while the other group was subjected to a recovery period on a standard chow diet for an additional 10 weeks (Recovery). The allocation of mice to experimental groups was performed randomly at the age of 3 weeks, ensuring that initial body weights were not statistically different among the groups.

During the study period, body weight was assessed weekly. The statistical analysis for identifying significant differences between the diets was conducted using analysis of variance (ANOVA) and post-hoc comparisons via Tukey's Honest Significant Difference (HSD) for each time point and sex. The weight loss associated with the recovery period was calculated by subtracting the body weight at 30 weeks from the body weight at 20 weeks, normalized to the body weight at 20 weeks.

Body composition analysis, specifically fat and lean mass, was determined at 13, 16, 20 and 24 weeks of age using the EchoMRI700™ instrument (Echo Medical Systems, USA). Statistical analysis was performed using ANOVA and post-hoc comparisons via Tukey's HSD test to identify significant differences in fat or lean mass per age and sex between the various diet groups.

For euthanasia, a lethal dose of isoflurane (Baxter Deutschland

GmbH, Germany) was administered, followed by cardiac puncture to collect serum samples for subsequent analysis. Mouse body weights, as well as the weights of key organs, including the liver, visceral, subcutaneous, and brown adipose tissues, were recorded during euthanasia. The organ weights were normalized to the overall body weight, and a Kruskal-Wallis test followed by Dunn's test was performed to identify significant differences between the groups for each tissue, sex, and subgroup (treatment and recovery). The organs were dissected and promptly cryopreserved using liquid nitrogen.

2.2. Histological characterization

Adipose tissue samples were fixed at room temperature in 4 % zinc formalin and subsequently embedded in paraffin. Sections of 10 μm thickness were mounted on glass slides, deparaffinized in xylol, and stained with hematoxylin (hematoxylin solution according to Gill II, Carl Roth GmbH + Co. KG, Germany) and eosin (eosin Y solution 0.5 % in water, Carl Roth GmbH + Co. KG, Germany). Liver tissues were embedded in OCT Embedding Matrix (Cell Path Ltd, United Kingdom) and frozen immediately.

A blinded analysis of the stained sections was conducted using a Keyence BZ-X800 microscope and the accompanying Keyence BZ-X800 Analyze 1.1.1.8r software (KEYENCE DEUTSCHLAND GmbH, Neu-Isenburg, Germany) to identify adipocytes and measure their size and perimeter in multiple sections.

2.3. Metabolomics sample preparation

DINCH, MINCH, and the secondary metabolites were quantified in the liver and adipose tissues by an adapted method described previously (Goerdeler et al., 2024). Briefly, tissues were extracted by an MeOH/chloroform/water (1:1:1) extraction. Each tissue was combined with MeOH (−20 °C) and ice-cold H_2O in a 1:1 ratio. Following lysis in a tissue lyser (Qiagen, Germany) at a frequency of 30 ms for 10 min, an equal amount of −20 °C cold chloroform was added, and the extraction mixture was shaken at 1,400 rpm and 4 °C for 20 min. Samples were centrifuged at 18,000 x g and 4 °C for 5 min, and 300 μL of the non-polar fraction was collected and evaporated to complete dryness (Concentrator plus, Eppendorf, Germany). The absolute tissue concentrations were approximated using an external calibration curve with extracted tissues conditioned with DINCH, MINCH, and the secondary metabolites. In detail, 50 mg of each tissue type (subcutaneous, visceral and brown adipose and liver tissue from HFD animals) was incubated for 2 h with 50 μL of a standard mix with different concentrations (100 μM, 50 μM, 25 μM, 10 μM, 5 μM, 1 μM, 500 nM, 100 nM, 10 nM, and 1 nM) and subsequently extracted by the above mentioned MeOH/chloroform/water (1:1:1) extraction. Quantification of the extracted samples was performed after first dissolving in 35 μL MeOH per 50 mg extracted tissue, then adding 35 μL H_2O per 50 mg extracted tissue. Mock extractions ruled out possible contamination by the extraction procedure and the solvents (data not shown).

2.4. Metabolite data acquisition

For the targeted LC-MS/MS measurement, 10 μL of each sample was injected into an Agilent 1290 II infinity UPLC system (Agilent Technologies Inc., USA) coupled online with a QTRAP® 6500 + system (AB Sciex, USA). Separation was achieved by using a Chromolith® Performance RP-18e column (2.0 x 100 mm, 1.5 μm, 130 Å; Merck, Germany) equipped with a Chromolith® RP-18e pre-column (2.0 x 5 mm; Merck, Germany) and application of the following gradient of solvent A (0.05 % formic acid in water) and solvent B (0.05 % formic acid in acetonitrile): 0 – 1 min 20 % B (flow rate of 0.4 mL/min), 1 – 2.5 min 20 – 50 % B, 2.5 – 6.5 min 50 – 95 % B, 6.5 – 10 min 95 % B (0.6 mL/min flow rate), 10 – 11 min 95 – 20 % B, and 11 – 13 min 20 % B (0.4 mL/min flow rate). The temperature of the autosampler and column oven were set to 8 °C and 40 °C, respectively.

Identification and quantification were based on a scheduled MRM method measured in positive (DINCH) and negative (MINCH) ESI ionization switch-mode. The limit of detection (LOD) and the limit of quantification (LOQ) for each analyte in the corresponding tissues were determined using the blank value approach (Little, 2015) and are listed in Supplemental Table 1. GraphPad Prism (v10.0, USA) and R (v4.05) were used for visualization and statistical analysis. Normality assumption of the data for performing ANOVA was assessed by using the D'Agostino/Pearson, Anderson-Darling and Shapiro-Wilk test and analyzing Q-Q plots of the residuals. As the Brown-Forsythe test indicated a difference between the standard deviations of the groups, significance was determined by Welch ANOVA followed by Dunnett's T3 post-hoc test with separate analyses for female and male mice. If HFD concentration values were below the LOD, a one-way *t*-test of the LD or HD group against the LOD was performed. In groups with missing values below the LOD, these values were imputed with a value equal to half of the LOD.

This data is available at the NIH Common Fund's National Metabolomics Data Repository (NMDR) website, the Metabolomics Workbench, https://www.metabolomicsworkbench.org, where it has been assigned Project ID PR002076. The data can be accessed directly via its Project at the Metabolomics Workbench: https://dx.https://doi.org/10.21228/M88G1K.

2.5. Glucose and insulin tolerance tests

Intraperitoneal (ip) glucose tolerance tests (GTT) and insulin tolerance tests (ITT) were performed at the age of 12, 18 and 28 weeks as described previously (Klöting et al., 2008). In brief, GTT was performed after an overnight fasting period of 16 h by injecting 2 g/kg body weight glucose and measuring the blood glucose levels after tail vein incision at 0 (baseline), 10, 30, 60, and 120 min after injection. ITT was performed in random-fed animals by injecting 0.75 unit/kg body weight human regular insulin (40 units Actrapid; Novo Nordisk, Denmark). Glucose levels were determined in blood collected from the tail tip immediately before and 15, 30, and 60 min after the intraperitoneal injection.

Data analysis was conducted to assess the impact of the diets on blood sugar levels across different time points during the ITT and GTT, considering variations by age and sex. For each unique combination of these variables, a Welch ANOVA followed by Dunnett's T3 post-hoc test was performed to identify significant differences in blood sugar levels between the various diet groups.

Furthermore, the area under the curve (AUC) has been calculated using the *trapez* function from the *pracma package* version 2.4.4 (Borchers, 2023) in R version 4.4.0 (R Core Team, 2023). The statistical significance of the results was calculated via ANOVA with Tukey's HSD as the post hoc test.

2.6. Quantification of serum adiponectin, leptin, insulin and C-peptide

Adiponectin, insulin, C-peptide and leptin levels were quantified in mouse serum using the following ELISA kits according to the manufacturer's instructions: Adiponectin Mouse ELISA (Adipogen Life Sciences, Switzerland), Mouse Ultrasensitive Insulin ELISA (ALPCO, USA), Mouse C–Peptide ELISA (ALPCO, USA), and Mouse/Rat Leptin Quantikine ELISA Kit (R&D Systems Europe, UK). Insulin secretion capacity was assessed using the insulin/C-peptide ratio to gain a better understanding of endogenous insulin production. For adiponectin, insulin, C-peptide and insulin/C-peptide ratio, ANOVA with Šidák post hoc was used for each sex and subgroup (treatment and recovery) to calculate statistical significance between groups. The Dunn test was used for leptin due to very low p-values in the test for normal distribution with the Shapiro test, especially in the female group.

2.7. Lipid analysis

Serum lipids, including triglyceride, total cholesterol, high-density lipoprotein (HDL) cholesterol, and low-density lipoprotein (LDL) cholesterol, were quantified from the serum samples collected during euthanization in the Institute of Laboratory Medicine, Clinical Chemistry and Molecular Diagnostics of University Leipzig (Germany). ANOVA with Šidák post hoc was used to test for statistical significance between groups for each measure, subgroup (treatment and recovery) and sex.

2.8. Triglyceride content of the liver

The triglyceride content of the liver was quantified in five randomly selected samples per group using the Triglyceride-Glo™ Assay (Promega Corporation, USA), following the manufacturer's instructions. In summary, 25 mg of liver tissue was homogenized in 1 ml of phosphate-buffered saline (PBS). The homogenate was diluted 1:100, and 25 µl of the dilution was mixed 1:1 with glycerol lysis solution and/or without lipase. The mixture was then incubated for 30 min at 30 °C while shaking. Subsequently, 50 µl of glycerol detection reagent was added and mixed manually. Following a 60-minute incubation period at room temperature, the luminescence was quantified. The concentrations of free and total glycerol were calculated using a standard curve. The triglyceride content was calculated as the difference between the total and free glycerol concentrations. ANOVA with post hoc Tukey HSD was employed for each sex in the treatment and recovery phases to ascertain the statistical significance between groups.

2.9. Metabolic characterization

Energy metabolism was analyzed by indirect calorimetry using the CaloSys v2.1 metabolic chamber (TSE Systems, Germany). The mean oxygen consumption, carbon dioxide production, energy expenditure and spontaneous locomotor activity were recorded at 5-minute intervals over 72 h. The body weight of the mice was also measured before and after their time in the metabolic chamber. Subsequently, the mice were permitted to recuperate for 48 h.

For energy expenditure (EE) and the respiratory exchange ratio (RER), mean values were calculated for the diurnal (lightness $>$ 50 %) and nocturnal (lightness $<$ 50 %) cycles, as well as for the total period. The dataset was structured for statistical analysis by categorizing variables, including measurement type (EE or RER), cycle, and sex. For each unique combination of these variables, a linear model was fitted with diet as the primary independent variable (Speakman, 2013). Body weight was used as a random intercept to account for variations among mice and to determine its influence on EE and RER. Post-hoc comparisons were performed using Tukey's HSD test to identify significant differences among the different diet groups.

2.10. Serum proteomic analysis

Plasma samples were analyzed by the Core Facility Metabolomics and Proteomics (CF-MPC) of the Helmholtz Munich (Germany) and the Institute of Laboratory Medicine, Clinical Chemistry and Molecular Diagnostics of University Leipzig (Germany) using the Olink® Target 96 Mouse Exploratory panel while applying the proximity extension assay technology. The resulting data was provided in Normalized Protein eXpression (NPX) values.

A linear mixed model using *lmer* from *lme4 package* version 1.1–35.3 (Bates et al., 2015) in R version 4.4.0 (R Core Team, 2023) was employed for the statistical analysis, which aimed to elucidate the impact of the diets on the biomarkers while accounting for potential interactions with biological variables such as sex and subgroup (treatment and recovery) differences across different proteins. The variability due to differences between the laboratories was considered a random factor in the overall analysis. To address the issue of multiple testing, the Bonferroni method was utilized. The significance threshold was 0.05, with a regulation estimate of |0.5|.

2.11. Proteomic sample preparation and data acquisition

Subcutaneous, visceral and brown adipose, as well as liver tissues, were lysed in urea buffer (20 mM HEPES pH 8.0 (Roth, Germany), 9 M urea (Merck, Germany), 1 mM sodium orthovanadate (Sigma-Aldrich, USA), 2.5 mM sodium pyrophosphate (Sigma-Aldrich, USA), 1 mM β–glycerophosphate (Alfa Aesar, USA)) in a pre–cooled tissue lyser (Qiagen, Germany) at a frequency of 30 ms for 5 min. Crude lysates were incubated for 30 min, and cell debris was removed by centrifugation at 16.000 x g and 10 °C for 15 min. The supernatants were transferred to new tubes, and protein concentration was determined using the Pierce™ 660 nm protein assay (Thermo Fisher Scientific, USA) according to the manufacturer's instructions.

20 µg protein per sample was reduced with 50 mM TCEP (Sigma-Aldrich, USA) at 55 °C for 1 h, alkylated with 100 mM IAA for 30 min at room temperature (RT) in the dark and proteolytically cleaved using trypsin in a 1:40 (enzyme:protein) ratio at 37 °C overnight, applying a paramagnetic bead approach. Tandem mass tag reagents (TMT10-plex™, Thermo Fisher Scientific, USA) were dissolved in ACN and incubated with the peptides for 1 h at RT. The labelling reaction was terminated with 5 % hydroxylamine and the different labels were united. Labelled peptides were desalted on beads, eluted in two fractions using 87 % ACN (v/v) with 10 mM ammonium formate at pH 10 for the first and water with 2 % DMSO for the second fraction before peptide fractions were dried completely using a SpeedVac concentrator (Eppendorf, Germany).

All samples were analyzed in data-dependent acquisition on a setup consisting of an Ultimate 3000 RS nano ultra-performance liquid chromatography system (Thermo Fisher Scientific, USA) coupled to a Q Exactive HF Hybrid Quadrupole Orbitrap mass spectrometer (Thermo Fisher Scientific, USA) equipped with a TriVersa NanoMate system (Advion, USA). Peptides were trapped on an Acclaim PepMap 100 C18 column, nanoViper, 3 µm, 75 µm × 2 cm column (Thermo Fisher Scientific, USA) and separated for analysis on an analytical reverse-phase Acclaim PepMap 100 C18, nanoViper, 3 µm, 75 µm × 25 cm column (Thermo Fisher Scientific, USA) at a flow rate of 0.3 µl/min. Peptides were eluted over a 180 min three–step linear gradient starting at 4 % solvent B (solvent A: 0.1 % FA in water; solvent B: 80 % ACN/0.1 % FA in water), *via* 30 % B after 100 min, 55 % B after 140 min reaching 99 % B after 155 min followed by flushing of the column for 5 min at 99 % B and subsequent equilibration to initial conditions. Settings for the acquisition of positive mode full MS scans were the following: scan range of 350–1550 *m/z*, AGC target of 3×10^6 ions, resolution of 120,000 and a maxIT of 120 ms. The top 15 precursor ions were selected for fragmentation, applying a 0.7 *m/z* isolation window and an NCE of 34 for CID fragmentation. Fragment ion spectra were recorded at the following settings: resolution of 60,000, maxIT of 150 ms, AGC target of 1×10^5 and a dynamic exclusion of 45 sec.

2.12. Protein database searches and tissue proteomics data analysis

Proteome Discoverer (2.5.0.400, Thermo Fisher Scientific, USA) was used to search raw files against the UniProtKB reference proteome of *Mus musculus* (downloaded 24.05.2022, 55,315 entries). Carbamidomethylation of cysteines (C) and TMT-labelling of lysines (K) were set as fixed modifications, while oxidation of methionine (M) and N–terminal acetylation and TMT-labelling were set as variable modifications. Two missed tryptic cleavages were allowed. The false discovery rate (FDR) for peptide and protein identifications was set to 0.01, using a target-decoy approach with a reversed decoy database. Proteins were considered to be identified by at least two peptides, one of which is unique, and the quantification was based on the intensities of all peptides. Only proteins found in at least three (BAT) or five (VIS AT, SC AT, liver)

independent biological replicates were considered for further analysis. The collected mass spectrometry proteomic data was deposited to the ProteomeXchange Consortium via the PRIDE partner repository (Perez-Riverol et al., 2019) with the dataset identifier PXD054970 and project DOI https://doi.org/10.6019/PXD054970.

R v3.6.1 was used for statistical analysis according to the workflow described for the R package *proteomicsr* version 1.0.0 (Karkossa, 2023). TMT reporter intensities were corrected to the internal reference standard (a pool of all samples), and data was $\log_2$ transformed. Mean intensities were computed to calculate fold changes (FC) for different dietary exposures. Significant changes were determined using a two-sided students *t*-test. A gene set enrichment analysis of all differentially abundant proteins (FDR < 0.05) was performed using the MSig database (MSigDB, gsea-msigdb.org/gsea/msigdb/collections.jsp) with the curated Reactome pathway database mouse gene sets for the different conditions (Milacic et al., 2024).

2.13. Statistical analysis

All information regarding the statistical data evaluation can be found in the respective figure legend. Generally, the data are presented as mean ± SD, if not stated otherwise and have been tested for normal distribution using the D'Agostino/Pearson, Anderson-Darling and Shapiro-Wilk tests, as well as Q-Q plots of the residuals. The comparisons considered included LD *vs* HFD, HD *vs* HFD and LD *vs* HD. As the focus of this study was on analyzing the effects of the chemical treatment, significant changes between SD and the HFD-diets (HFD, LD and HD) were not displayed in the figures. When the data were not normally distributed, a Kruskal-Wallis test with a Dunn post hoc test was conducted to ascertain the significance values between groups. When the data were found to be normally distributed and exhibited equal variance, initially tested by a Brown-Forsythe test, an ANOVA with a Šidák post hoc test was conducted. If the data demonstrated no equal variance, a Welch ANOVA followed by a Dunnett's T3 post hoc test was performed. In the case of metabolomic data, if the concentration values for the HFD were below the LOD, a one-way t-tests of the LD and HD groups were conducted with LOD serving as the control. The serum proteome was analyzed using a linear mixed-effects model with a Bonferroni correction for multiple testing, whereas the tissue proteome was analyzed using a two-sided Student's *t*-test. All analysis has been performed separately for both sexes and dietary phases (treatment/recovery).

3. Results

3.1. Dietary intake of DINCH does not affect body weight and adipose tissue distribution in C57BL/6N mice

Mice were fed high-fat diets containing two doses of DINCH (low dose: LD 4,500 ppm; high dose: HD 15,000 ppm) for 16 weeks of treatment following 10 weeks of recovery (Fig. 1A). Weekly weight measurements during the treatment and recovery phase confirmed the efficacy of the high-fat diet (HFD) in female and male mice (Fig. 1B and C) by significantly increased bodyweight at age of 20 weeks (Supplemental Table 11). Since this study focused on analyzing the effects of the chemical treatment, other significant changes between SD and the HFD-diets are not displayed in the following figures.

A significant difference in body weight between the DINCH diets was

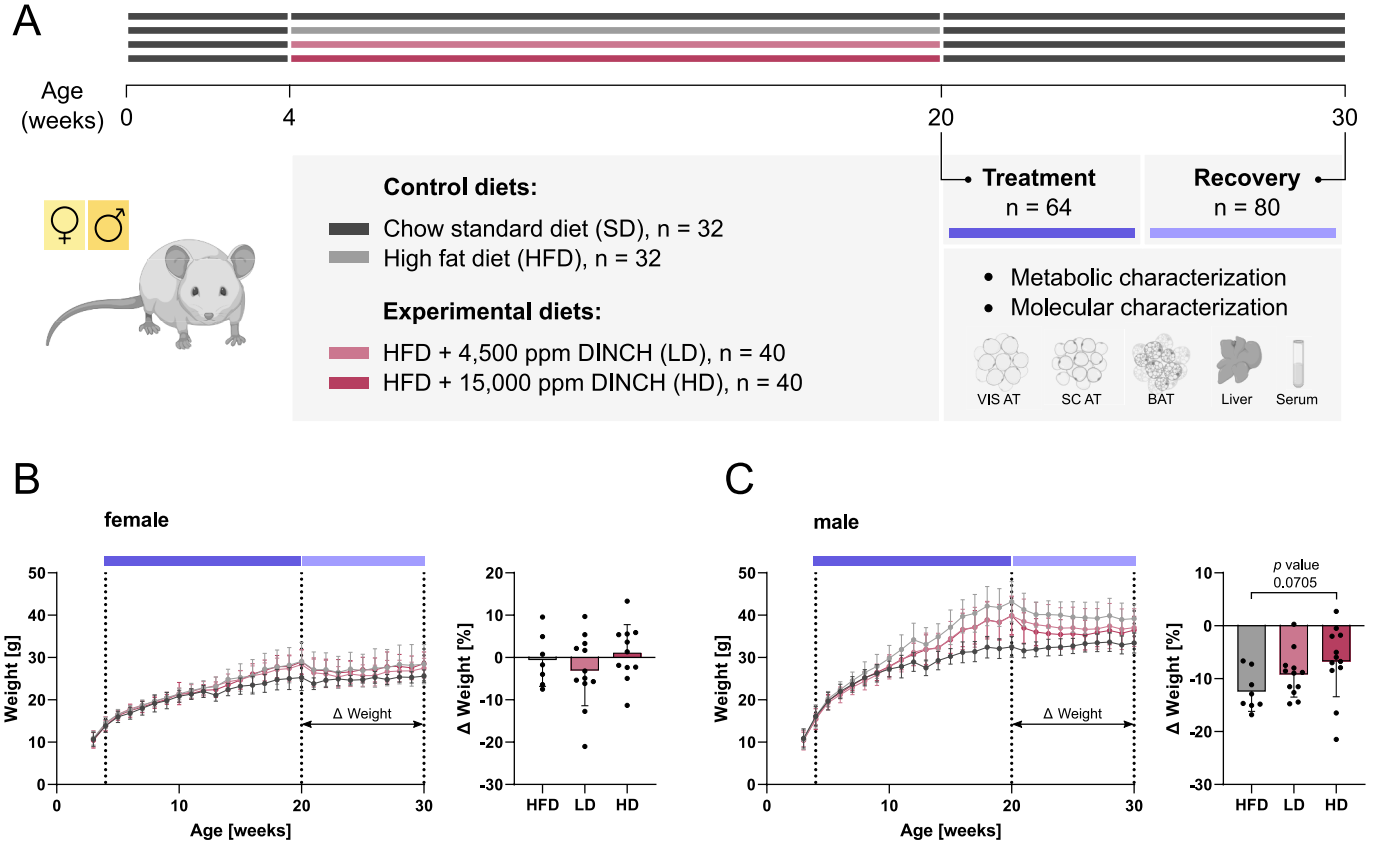

Fig. 1. Experimental set up and body weight development. (A) Experimental set up and definition of sub groups with equal numbers of males and females in each. Detailed overview of group distribution is provided in Supplemental Table 2. Body weight was measured weekly and is presented for (B) female and (C) male mice. The weight loss during the recovery time was calculated by subtracting the body weight at 30 from the weight at 20 weeks of age, normalized to the weight at 20 weeks. Significant changes in body-weight data are displayed in Supplemental Tables S11. Significance was calculated using ANOVA and Šidák post hoc tests and data is presented as mean ± SD.

not observed at the endpoints at ages 20 and 30 weeks, except for the HD to HFD comparison at age 30 weeks. Mice receiving DINCH-containing HFD showed overall lower body weights compared to HFD, however this was not significant (Fig. 1B and C). Notably, this trend was more prominent in males (Fig. 1C) than in females (Fig. 1B). During the recovery phase a trend of weight loss emerged in the HFD, LD and HD fed male mice, which was most pronounced for the HFD subgroup (Fig. 1C). The male LD and HD groups showed a lower weight loss response during recovery SD feeding (Fig. 1C). The fat and lean mass were quantified by EchoMRI measurement at the ages of 13, 16, 20 (treatment phase) and 24 (recovery phase) weeks (Supplemental Fig. 1). However, the ingestion of DINCH did not elicit any discernible effects.

To further assess potential effects of the diets on the body composition, the relative weights of the liver and three adipose tissue depots

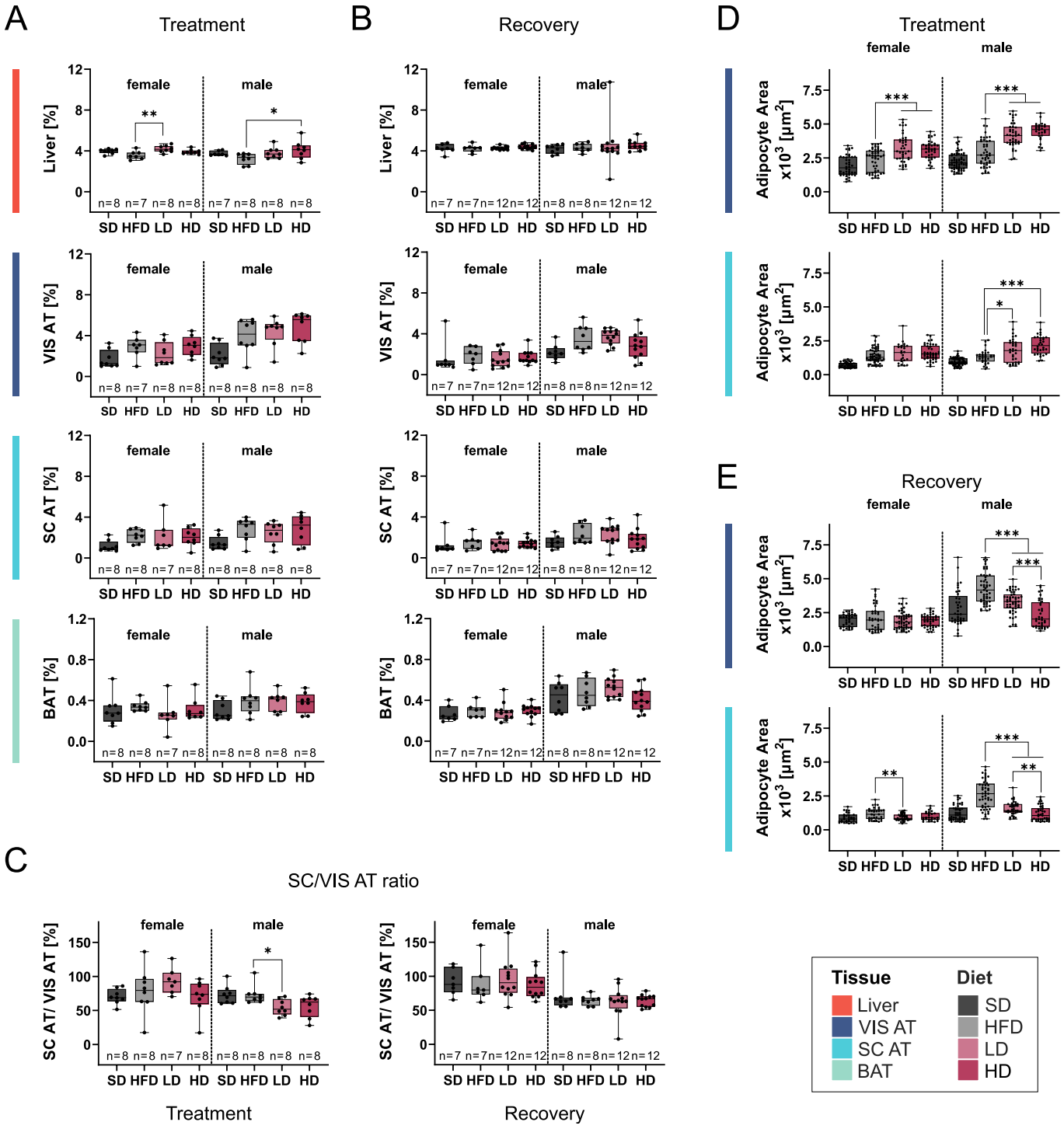

Fig. 2. Relative content of liver and adipose tissue depots, their ratio and respective adipocyte area. Organ weight relative to body weight is shown staggered according to sex and experimental phase (A, treatment; B, recovery) for liver, subcutaneous (SC AT), visceral (VIS AT) and brown adipose tissue (BAT). (C) Ratio of SC/VIS AT. Quantified adipocyte areas from histological analysis of VIS and SC AT after (D) treatment and (E) recovery (n = 24–59). Statistical significance was calculated using a Kruskal-Wallis with a Dunn post hoc test. Significant changes between SD *vs* HFD are not displayed. Adjusted p values are indicated as * $p < 0.05$, ** $p < 0.01$, *** $p < 0.001$. Data is presented as median with whiskers indicating minimum and maximum datapoints.

(visceral, subcutaneous and brown) were analyzed.

The ingestion of DINCH did not result in any significant alterations in the relative organ weights of SC AT, VIS AT, or BAT in either sex (Fig. 2). However, an increase was observed in the liver of LD-fed female and HD-fed male animals at 20 weeks of age (Fig. 2A). During the recovery phase, no significant effects of DINCH in the relative organ weights were discerned in either sex (Fig. 2B). Analysis of the ratio of subcutaneous to visceral adipose tissue showed a significant reduction in the LD group of males (Fig. 2C), which was due to a non-significant increase in VIS AT and a decrease in SC AT by the DINCH diet.

A histological analysis of VIS and SC AT revealed alterations in adipocyte area in response to DINCH feeding (Fig. 2D and E). In SC AT the effect of DINCH were concentration-dependent in males, whereas no effects were observed in females. In VIS AT, dietary DINCH exposure significantly increased adipocyte area in both sexes, irrespective of concentration (Fig. 2D). Following the recovery period (Fig. 2E), adipocyte area was significantly increased in males in the HFD-fed group compared to the treatment phase in both SC AT and VIS AT. In contrast, adipocyte areas after recovery were significantly reduced in DINCH-treated female and male mice and were lower compared to the HFD-

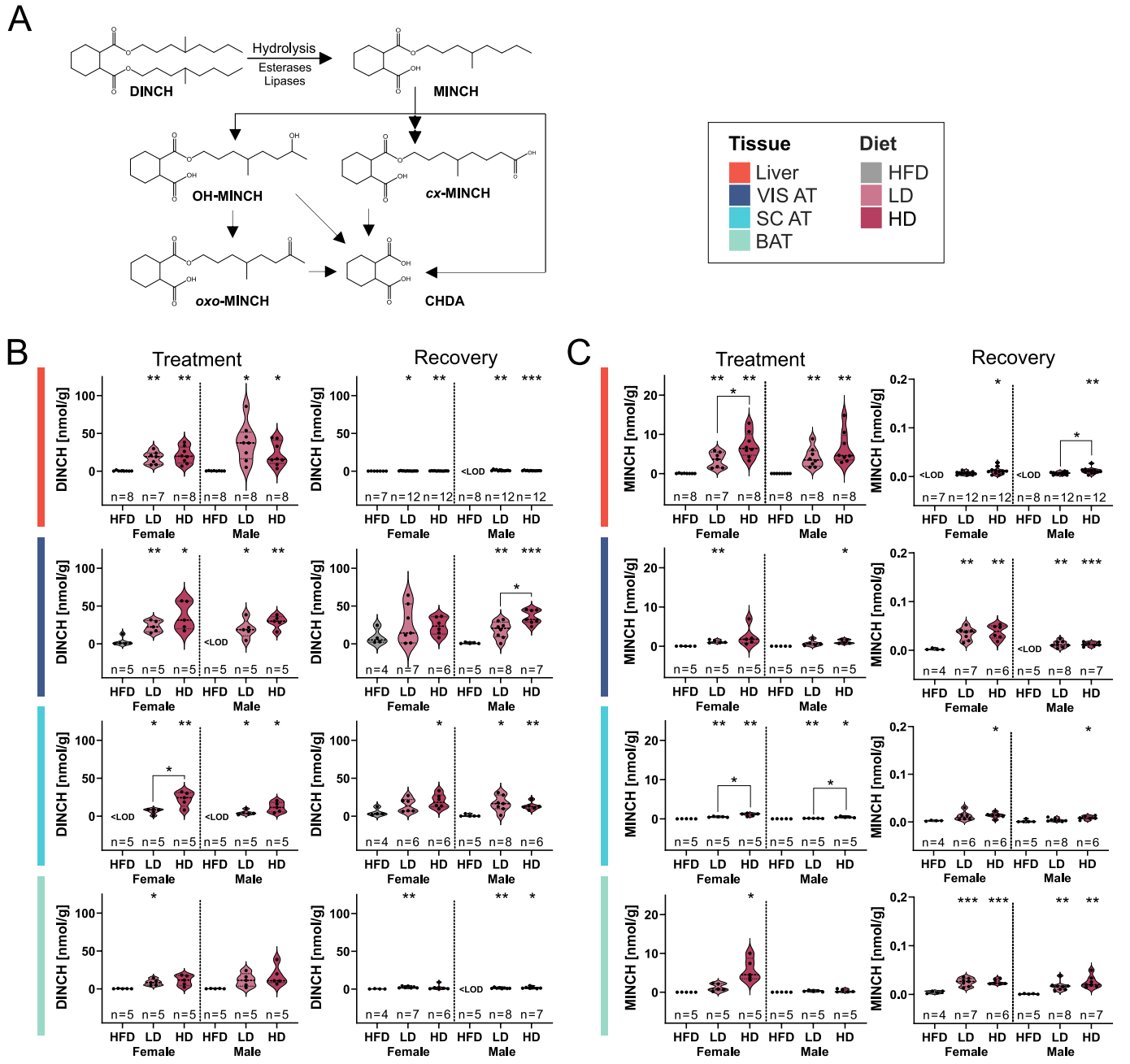

Fig. 3. Analysis of concentrations of DINCH and MINCH in adipose tissues and liver. Analysis of exposure concentrations of DINCH and MINCH in mice tissues. (A) General overview of the biotransformation of DINCH to MINCH, the secondary metabolites OH-MINCH, cx-MINCH, oxo-MINCH and CHDA (scheme adapted from Schütze et al. (2012)). (B) Concentrations of DINCH measured in the liver, VIS AT, SC AT and BAT of mice after 16 weeks of feeding with HFD containing DINCH (Treatment) followed by 10 weeks feeding with standard chow (Recovery). During treatment mice were fed with a low dose (LD: 4,500 ppm) and high dose of DINCH (HD: 15,000 ppm) and compared to mice fed with high-fat diet only (HFD). (C) Concentrations of MINCH measured in the liver, VIS AT, SC AT and BAT of mice in the Treatment and Recovery group. Data in (B) and (C) are presented as absolute concentrations (nmol/g tissue). Tissue concentrations of secondary metabolites can be found in Supplemental Fig. 2 and 3. Significant differences were calculated by Welch ANOVA followed by Dunnett's T3 post-hoc test (female and male separated) or by one-way test against the LOD if the HFD concentration values were below LOD; p values are indicated as * $p < 0.05$, ** $p < 0.01$, *** $p < 0.001$.

fed group (Fig. 2D and E).

3.2. DINCH and MINCH reach adipose and liver tissues with levels being partially retained during recovery period

To determine the consequences of dietary DINCH exposure, we evaluated the distribution of DINCH and its metabolites in different tissues. The concentrations of DINCH, MINCH and the secondary metabolites OH-MINCH, oxo-MINCH and cx-MINCH were measured in the liver and three adipose depots (VIS AT, SC AT, BAT) of the treatment (Treatment) and recovery group (Recovery) in male and female mice (Fig. 3A and Supplemental Fig. 2). The concentration levels were compared to those of mice fed with HFD alone. To relate the measured concentrations to the amount of feed ingested, feed intake was quantified in the metabolic chamber (data not shown). However, due to methodological problems in the measurement of feed intake, which resulted in considerable deviations in the measurement these data could not be used.

After treatment, DINCH was detected at the highest concentrations in all tissues in both females and males (10.7 – 31.4 nmol/g HD; Fig. 3B), followed by MINCH (0.14 – 6.4 nmol/g HD; Fig. 3C). The secondary metabolites were found in the liver at similar (OH-MINCH) or 5-fold lower concentrations (oxo-MINCH and cx–MINCH) compared to MINCH, and only traces were found in the various adipose depots (Supplemental Fig. 2). In general, the concentrations of DINCH, MINCH and secondary metabolites showed high inter- and intra-individual variability within the measured tissues in both females and males (Fig. 3B and C, Supplemental Fig. 2).

The concentrations of DINCH did not differ significantly between the tissues. However, there was a trend towards higher concentrations in VIS AT and liver compared to SC AT and BAT, particularly in the low dose exposure group (Supplemental Fig. 3). In contrast to DINCH, MINCH concentrations were higher in liver than in adipose tissue depots (Supplemental Fig. 3). Interestingly, MINCH concentrations were higher in females than males, especially in the HD group of BAT (females HD 4.5 nmol/g; males HD 0.15 nmol/g; Fig. 3C and Supplemental Fig. 3). After recovery, DINCH concentrations were notably reduced in the liver and BAT (111-fold and 9-fold, respectively), but not in the VIS AT and SC AT (Fig. 3B; Supplemental Fig. 3 and 5). In contrast, the concentrations of MINCH and the secondary metabolites were reduced to trace levels in all tissues after the recovery phase (Fig. 3C, Supplemental Figs. 2, 3 and 4).

3.3. Dietary DINCH uptake affects insulin sensitivity but not glucose tolerance in a sex-specific manner

To identify early alterations of insulin sensitivity or glucose tolerance induced by DINCH in HFD, we performed intraperitoneal insulin and glucose tolerance tests (*i.p.* ITT and GTT) in 18-week-old mice during treatment, and in 28-week-old mice to assess the recovery phase (Fig. 4).

Under high-fat conditions with DINCH during treatment phase, female mice exhibited impaired insulin sensitivity at the whole-body level (Fig. 4A) compared to high-fat fed control animals. No differences could be detected in the 18-weeks old males (Fig. 4B, Treatment), where all animals showed insulin resistance regardless of the feeding. In the recovery phase, impaired insulin sensitivity was reversed in all female groups except the HFD group (Fig. 4A). Males, on the other hand, showed a slight improvement in insulin sensitivity during recovery phase (Fig. 4B). Interestingly, glucose tolerance did not differ in the females during treatment period (Fig. 4C).

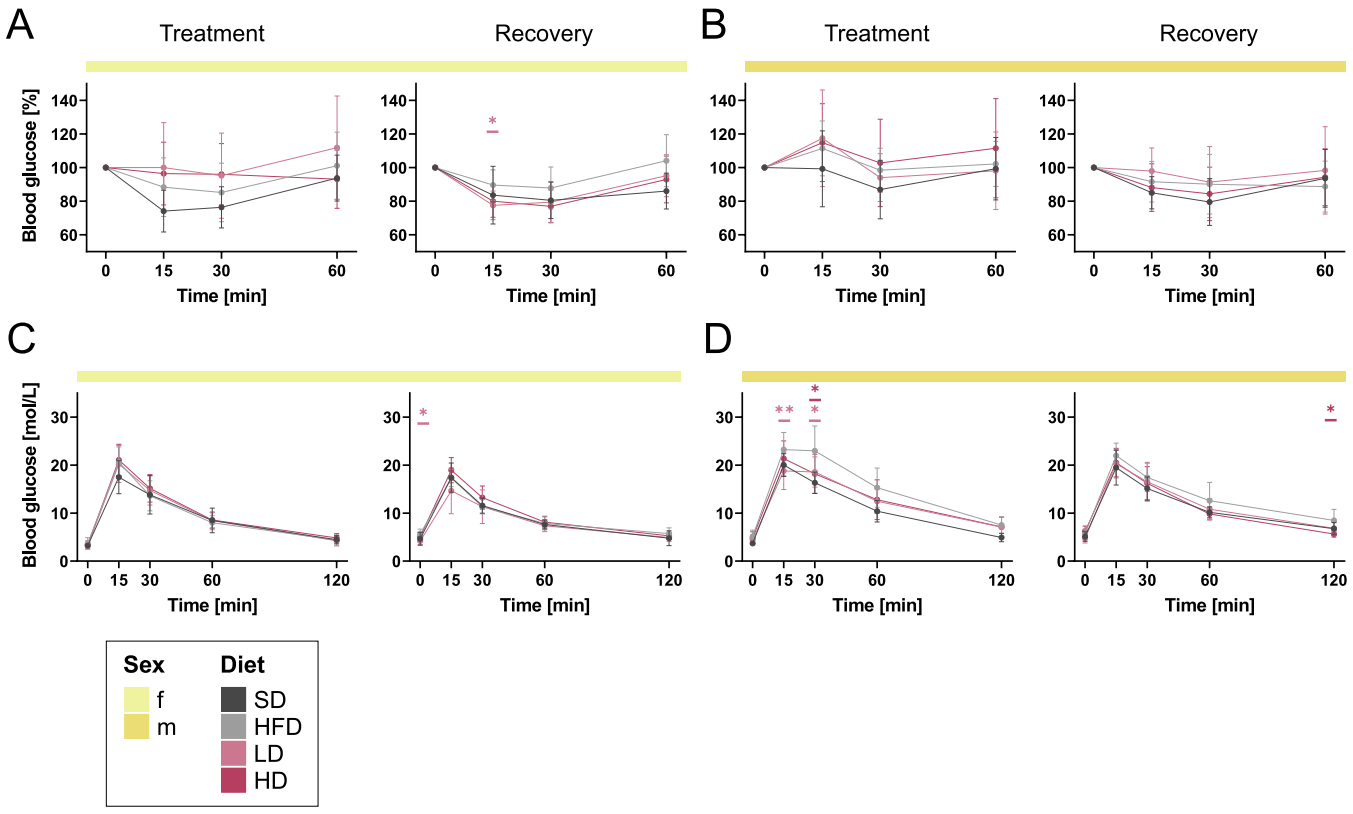

Fig. 4. Glucose and insulin tolerance. For the insulin tolerance test (ITT), blood glucose levels were monitored for 60 min and normalized to the initial blood glucose level at t = 0 at during treatment (18 weeks) and recovery (28 weeks) in (A) female and (B) male mice. For the glucose tolerance test (GTT), blood glucose levels were monitored for 120 min at treatment (18 weeks) and recovery (28 weeks) weeks in (C) female and (D) male animals (n = 5–21). Statistical analysis was conducted for each time point between the HFD groups using Brown-Forsythe and Welch ANOVA tests. Significant changes between SD *vs* HFD are not displayed. *p* values are indicated for LD and HD compared to HFD as * $p < 0.05$, ** $p < 0.01$, *** $p < 0.001$.

In males, glucose tolerance was slightly impaired in HFD animals (Fig. 4D), as can be seen from the 15- and 30-minute time point. At 30 min, the curve did not flatten, indicating impaired glucose tolerance. This glucose intolerance was reversible in the recovery phase (Fig. 4D).

To complete the analysis and quantify the overall response, area under the curve values were calculated, that did not indicate significant differences (Supplemental Fig. 6).

3.4. Dietary DINCH exposure affects serum insulin, adipokines and lipid profile

To comprehensively understand the metabolic and endocrine effects of DINCH exposure during HFD, we measured serum concentrations of insulin and C-peptide, as well as adipokines, such as adiponectin and leptin. During the treatment period, no effect was observed for HFD containing DINCH compared to control HFD. Following the recovery period, there was a notable decline in insulin levels of LD and HD female

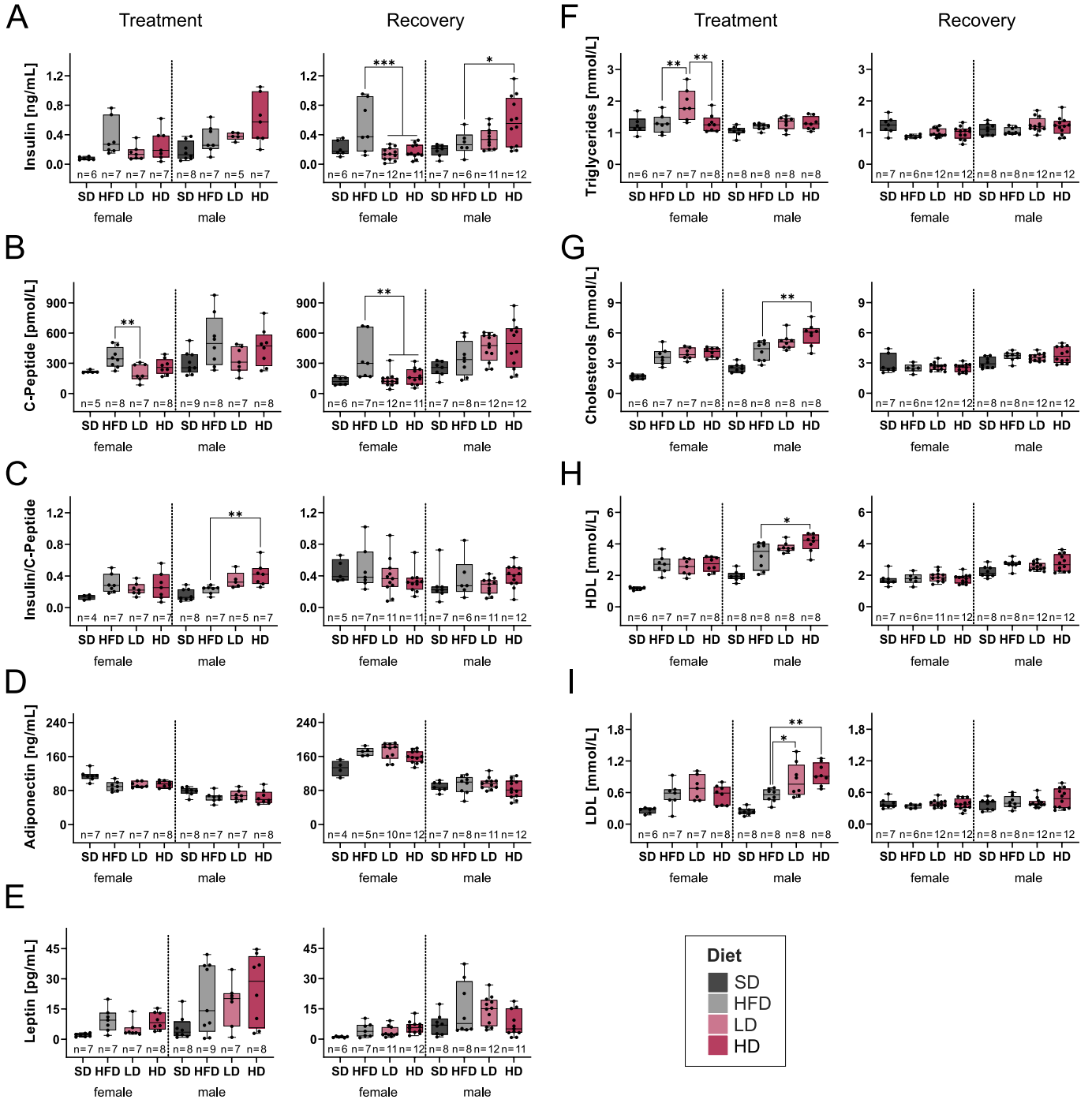

Fig. 5. Serum insulin, C-peptide, adipokine and lipid analysis. (A) Insulin, (B) C-peptide, (C) the ratio between insulin and C-peptide for endogenous insulin production, (D) adiponectin, (E) leptin, (F) Triglycerides (TGA), (G) overall cholesterol, (H) high-density lipoprotein (HDL) and (I) low-density lipoprotein (LDL) levels were measured in females and males after treatment and after recovery. Statistical significance between groups was calculated using an ANOVA with Šidák post hoc test and p values are indicated as * $p < 0.05$, ** $p < 0.01$, *** $p < 0.001$. Significant changes between SD *vs* HFD are not displayed. Data is presented as median with whiskers indicating minimum and maximum datapoints.

animals in relation to the HFD. In males, insulin serum levels were increased in DINCH exposed HD–fed animals. C-peptide levels (Fig. 5B) exhibited a comparable pattern to insulin in females, with notable reductions in the LD compared to the HFD group. This was maintained throughout the recovery phase, with significance observed between the LD and HD compared to HFD–fed animals. In males, no significant effect of DINCH was observed. To gain a deeper insight into endogenous insulin production, the insulin/C-peptide quotient was assessed (Fig. 5C). While no significant effect was observed in females during the treatment period, male HD mice exhibited an increased quotient in relation to HFD-fed mice. Following recovery, no significant effects were observed in either sex due to dietary DINCH exposure.

To assess possible imbalances in lipid metabolism, the concentration of triglycerides (TGA), cholesterol, high-density lipoprotein (HDL), and

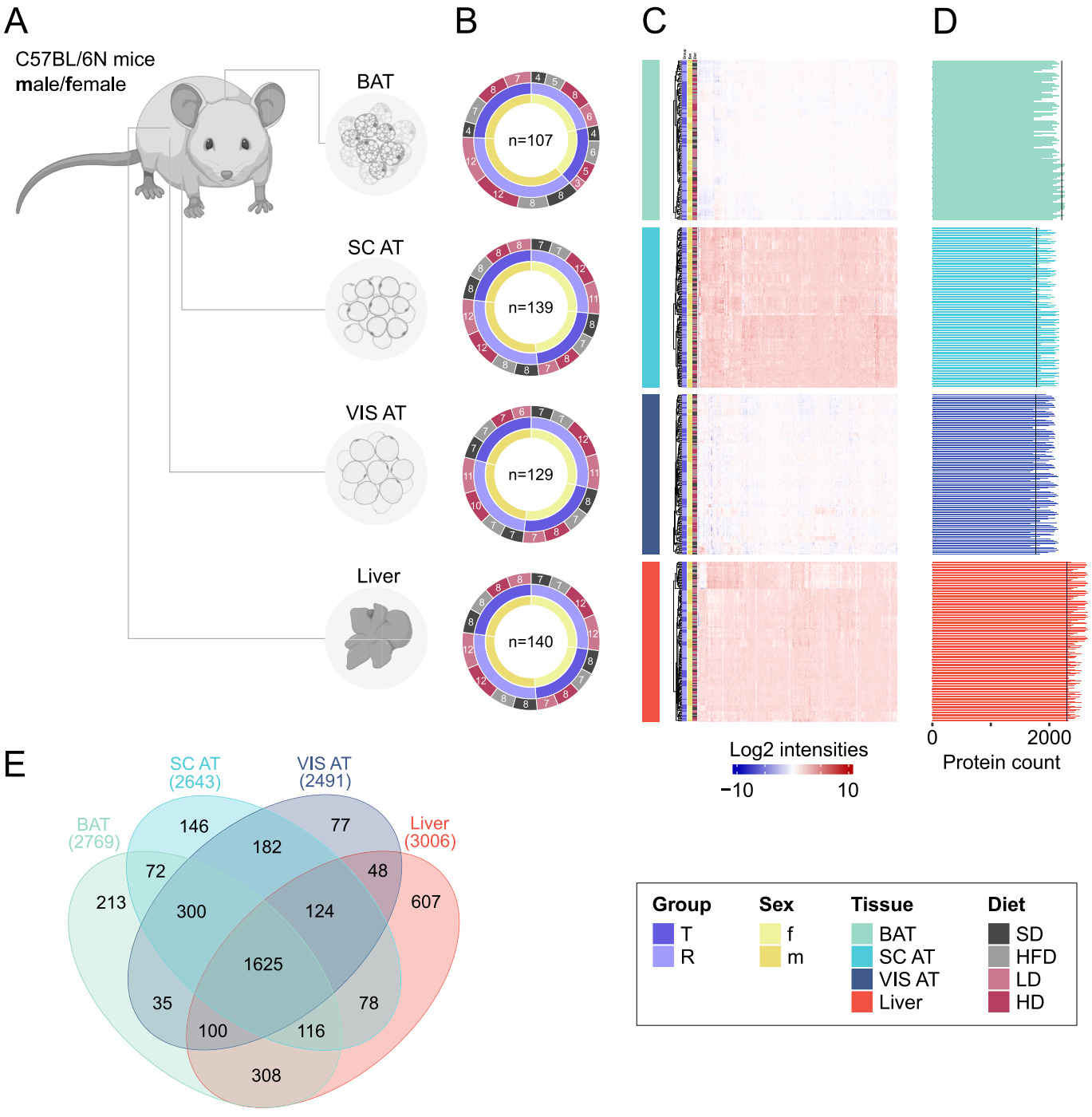

Fig. 6. Overview about the tissue proteome datasets. (A) Schematic overview of the tissues analyzed. Analyzed were visceral (VIS AT), subcutaneous (SC AT) and brown adipose tissue (BAT) as well as liver tissue. (B) Sample sizes are indicated by tissue, with subgrouping by sex (male/female, inner circle), group (treatment/recovery, 2nd circle) and diet during treatment phase (outer circle, SD/HFD/LD/HD). (C) Tissue wise hierarchical clustering of protein abundances across all samples using the R package *pheatmaps* with default clustering based on Euclidian distance. Dendrograms show sample clustering and the subgroups are indicated with the three layers of coloured headers. (D) Bar plots show the numbers of proteins for all samples after filtering for reliable quantification. The vertical line indicates the number of proteins found in > 50 % of all relevant comparisons made. (E) Venn diagram indicating overall, shared and specific proteins of the four tissues analyzed. SD, standard diet; HFD, high-fat diet; LD, HFD with low dose of DINCH 4,500 ppm; HD, HFD with high dose of DINCH 15,000 ppm.

low-density lipoprotein (LDL) was quantified in serum samples (Fig. 5F to I). In general, the lipid profiles exhibited a sexual dimorphism. DINCH treatment resulted in elevated levels of total, HDL–, and LDL–cholesterol in males (Fig. 5G to I), with these levels returning to initial levels during the recovery period. In females, circulating triglycerides were elevated in the LD group, while trends are reversible following the recovery phase (Fig. 5F). The overall cholesterol levels, as well as those of HDL and LDL, were not affected by the DINCH diet in females (Fig. 5G to I). In conclusion, the administration of DINCH has been demonstrated to exert a sex-specific influence on circulating lipids. The measurement of triglycerides in the liver did not indicate any notable effect of DINCH exposure (Supplemental Fig. 7).

3.5. Metabolic characteristics of DINCH fed animals do not differ from HFD control mice

To assess the effects of DINCH on metabolism, a basal metabolic rate measurement was carried out for 72 h in a metabolic chamber before euthanasia. The characterization of metabolic responses in a metabolic chamber represents a fundamental aspect of obesity research (Jéquier, 1989; Müller et al., 2016), as it enables the precise measurement of energy expenditure (EE) and the respiratory exchange ratio (RER). As a value for the total energy requirement of an organism, EE provides information on the effects of nutritional measures on the energy balance. The RER, defined as the ratio of carbon dioxide produced to oxygen consumed, reflects the predominant substrate being oxidized. Values closer to 0.7 suggest fat oxidation, while around 1.0 indicate carbohydrate oxidation (Ferrannini, 1988). Our findings demonstrate that RER was, significantly decreased some in some HFD–fed subgroups compared to SD-fed mice (Supplemental Fig. 8), but DINCH showed no significant effects. After the 10-week recovery phase, the HFD-based diets approach SD fed animals.

Similarly, EE was higher in HFD-than in SD (Supplemental Fig. 9), but again there were no significant effects of the DINCH diets. After the recovery period, the EE values of LD, HD and HFD approached the EE values of SD in females and in males (Supplemental Fig. 9).

3.6. Tissue and serum proteome profiles are affected by DINCH exposure and display changes in energy metabolism and immune response

For a comprehensive analysis of the tissue proteomes following dietary DINCH exposure, brown, subcutaneous and visceral adipose tissues (BAT, SC AT, VIS AT) as well as liver tissues were collected (Fig. 6A). Group sizes differed slightly due to limited sample availability or exclusion, resulting in overall n = 107 BAT, n = 139 SC AT, n = 129 VIS AT and n = 140 liver samples with subgroup sizes of n = 3 to n = 12 (Outer shell, Fig. 6B). We used a quantitative proteomics approach to analyze group-specific alterations in protein signatures from 4032 proteins that were reliably identified across all tissues in at least five replicates per experimental group for SC AT, VIS AT and liver, and at least three replicates for BAT samples due to the lower overall sample size. A hierarchical clustering and dimensionality reduction by principal component analysis (PCA) of all reliably quantified proteins per tissue showed a limited grouping of the experimental conditions (Fig. 6C and Supplemental Fig. 10). Main drivers behind the clustering were the sample origin in terms of group (treatment or recovery) and sex (female or male). Comparable numbers of proteins were detected in the four different tissues, with the largest set represented by 3,006 liver proteins followed by 2,769 BAT, 2,643 SC AT and 2,491 VIS AT proteins, and comparable numbers that remained for downstream analysis (Fig. 6D and E). A core of 1625 proteins was common to all tissues, while the liver proteome showed most unique proteins alongside and more overlapping proteins were found between the three adipose depots (Fig. 6E).

Comparing the tissues of lower (LD) and higher (HD) dose exposed mice to control HFD fed mice tissues, the proteome signatures of BAT, SC AT, VIS AT, and liver tissues showed mild changes with a low percentage of proteins displaying significantly altered abundances upon exposure (Fig. 7A). A pathway enrichment based on all proteins with a statistical change in abundance after DINCH treatment using the *Reactome* gene sets of the *Molecular Signatures Database* (MSigDB) indicated the involvement of pathways related to translation (*translation, regulation of expression of SLITs and ROBOs*), intermediary metabolism (*metabolism of amino acids and derivatives, TCA cycle and respiratory electron transport ATP synthesis*) and immune response (*CTLA4 inhibitory signalling, neutrophil degranulation*) in female and male BAT, mostly consistent in both treatment groups (Fig. 7B). Enriched regulatory pathways in SC and VIS AT of female and male mice comprised primarily pathways of the central energy and lipid metabolism (*metabolism of amino acids and derivatives, fatty acid, branched-chain amino acid and triglyceride metabolism, TCA cycle and respiratory electron transport*), cellular stress (*DNA damage telomere stress induced senescence, base excision repair AP site formation, defective intrinsic pathways for apoptosis*) as well as immune responses (*interleukin 12 signalling*). Specifically, in VIS AT from male mice pathways related to DNA and mRNA processing (*DNA methylation, mRNA splicing*) also appeared enriched. Liver tissues from female mice were enriched for mitochondria-associated central metabolism (*TCA cycle and respiratory electron transport ATP synthesis, fatty acid metabolism, CHREBP metabolic gene expression, cristae formation*), while those of male mice showed enriched pathways that are primarily associated with phase I drug metabolism (*xenobiotics, phase I functionalization of compounds, cytochrome P450 arranged by substrate type*) (Fig. 7B; see Supplemental Fig. 11 to 12).

In addition to the tissue proteomes, we analyzed the serum proteome using an Olink® Target 96 Mouse Exploratory panel. Except for the subgroup female HD, the analysis indicated candidates with significantly altered abundance and a log2 (fold change) above +/- 0.5 in all exposure groups (Fig. 7C). Candidates that were consistently found in at least two different treatment groups were interleukin–1 alpha (Il1a), C–C motif chemokine 3 (Ccl3), transforming growth factor beta–1 (Tgfb1) (downregulated) and interleukin–17A (Il17a, upregulated) (Fig. 7C). Except for Tgfb1, which usually originates from adipose tissue, Il1a, Il17a, and Ccl3 are pro-inflammatory and chemotactic cytokines of the immune system. An assignment of all proteins, with a log2 (fold change) above +/- 0.5, further considered regulated upon DINCH exposure, to their tissue or system of origin, indicates the immune system as the primary origin of altered proteins, followed by adipose tissue, endocrine system, lung and non-specific origins (Fig. 7D).

4. Discussion

Previous *in vitro* studies have demonstrated that the DINCH metabolite MINCH activates PPARγ, thereby inducing adipocyte differentiation and lipid accumulation, but also adipocyte dysfunction (Goerdeler et al., 2024; Schaffert et al., 2022; Useini et al., 2023). In contrast, *in vivo* rat studies did not reveal changes in body weight or lipid metabolism in response to DINCH exposure (Langsch et al., 2018). However, these studies did not assess organ-specific metabolic disruptions, such as fat depot distribution or adipokine secretion.

Here, we examined how DINCH affects metabolic and molecular alterations *in vivo* in a diet–induced obesity mouse model. Two doses of DINCH were administered to C57BL/6N mice for 16 weeks, after which a 10-week recovery period was allowed. After sixteen weeks of treatment, DINCH was detected in liver and adipose tissue and at the highest concentrations compared to the metabolites in C57BL/6 mice (Fig. 3B), confirming that it reached the tissue depots. Analysis of the metabolites in the treatment group showed that MINCH, besides OH-MINCH, was the predominant metabolite in the liver and the only metabolite in adipose tissue (Fig. 3C, Supplemental Fig. 2). A comparison of these tissue concentrations to existing data is difficult, as detailed concentrations of DINCH and the metabolites in liver and fat depots have not been reported yet. In approval studies, MINCH and the glucuronide of MINCH were similarly detected as primary metabolites in the feces and bile of

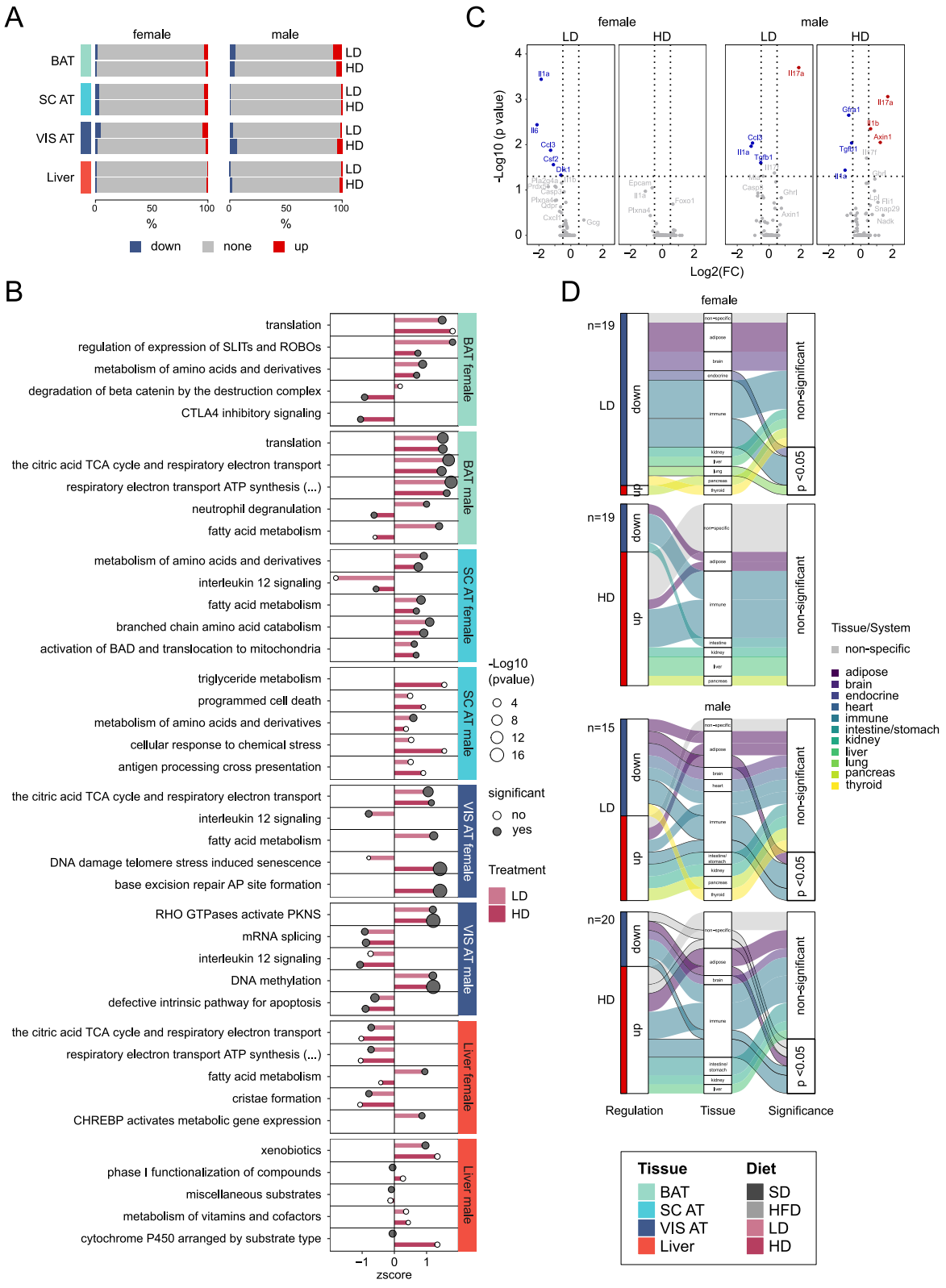

Fig. 7. Tissue and serum proteome regulation in the treatment groups. (A) Percentages of tissue proteomes of male and female mice with significant changes in protein abundance following dietary exposure to lower and higher levels of DINCH. (B) Pathway enrichment using the *Reactome* gene sets. Shown is a selection of the top enriched pathways of every tissue (male and female) based on significance, redundancy and relevance for both exposure conditions. Indicated are median log2 (fold changes), significance (p value < 0.05) and $-\log10$ (p values). (C) Volcano plots of the serum proteome Olink results separated by subgroups illustrate the most important candidates with significantly altered abundance after dietary exposure to DINCH. (D) Tissue origins of the regulated (absolute log2(fold change) > 0.05) serum proteins of male and female LD and HD subgroups, with intersects for the direction of regulation, the originating tissue or cellular system and the statistical significance.

Wistar rats, respectively, but not in the urine (Bhat et al., 2014; European Food Safety Authority (EFSA), 2006).

The analysis of tissue concentrations after the recovery period showed a substantial reduction of MINCH and the secondary metabolites to trace levels (Fig. 3C, Supplemental Fig. 2,4 and 5). For DINCH, a strong reduction of concentrations in the liver and BAT was observed, but no reduction in VIS AT and SC AT (Fig. 3B and Supplemental Fig. 4 and 5). This suggests potential bioaccumulation in these adipose tissue depots. Although approval studies showed a longer half-life in adipose tissue compared to liver and plasma after administration of 20 mg/kg body weight or 1,000 mg/kg body weight of radiolabeled DINCH to Wistar rats, no bioaccumulation was observed (Bhat et al., 2014; Langsch et al., 2018). Similarly, analysis of the metabolism of DINCH in humans after a single dose indicates rapid metabolism and excretion of DINCH (Koch et al., 2013). Notably, the concentrations of DINCH in these studies were determined after a single oral administration. In contrast, we analyzed the concentrations sixteen weeks after dietary exposure to DINCH. This is particularly relevant as other experiments in mice showed that after repeated exposure to the polybrominated diphenyl ether BDE 47, higher concentrations were observed in adipose tissue than after a single exposure (Staskal et al., 2006). Although the DINCH concentrations used in our experiment fall within the range of doses used in toxicokinetic studies with Wistar rats, they are relatively high and meet or exceed the NOAEL determined in the 13-week study performed according to OECD guideline 408 (1,500 ppm or 107 mg/kg bw/d for males and 4,500 ppm or 389 mg/kg bw/d for females; EFSA derived NOAEL 100 mg/kg bw/d) (Bhat et al., 2014; Anses (on behalf FR-MSCA), 2016).Consequently, no conclusions about the bioaccumulation potential at lower DINCH doses can be drawn, underlining the need for further evaluation of the bioaccumulation potential of DINCH, but also other phthalate alternatives. In particular, concentrations of DINCH and its metabolites in human serum are lacking, which could help to improve existing physiologically based pharmacokinetic (PBPK) models to better approximate human tissue concentrations (McNally et al., 2019).

With evidence that DINCH is deposited in tissue, further phenotypic characteristics were subsequently examined. A notable sex difference in body weight gain was observed in response to the HFD, with females demonstrating a smaller increase in body weight compared to males (Fig. 1B and C). This finding is consistent with the existing literature, which shows sex-specific differences in response to a high-fat diet in Sprague-Dawley rats and C57BL/6 mice, likely due to variations in metabolic and hormonal responses (Maric et al., 2022; Yang et al., 2014). Male mice on DINCH diets exhibited a slightly reduced weight gain compared to those on the control HFD diet (Main Supplemental File). Despite the potential expectation of weight gain due to the PPARγ–activating properties of the primary DINCH metabolite MINCH, which is well described for increased adipogenesis and lipid accumulation in *in vitro* models (Bereketoglu et al., 2024; Campioli et al., 2017; Goerdeler et al., 2024; Schaffert et al., 2022), this increase did not occur *in vivo*. Furthermore, there was no alteration in the distribution of lean and adipose tissue mass, nor specific fat depots such as subcutaneous, visceral, and brown adipose tissue (Fig. 2, Supplemental Fig. 1). A significant increase in relative liver content was observed in female mice due to the LD diet (Fig. 2A), which is consistent with previous findings in female rats showing even a doubling of liver weight after exposure to DINCH (Bhat et al., 2014), applying the same concentration range as in our study. Although no impact of DINCH on body weight gain compared to HFD-feeding was observed, adipocyte areas suggest that DINCH exposure increased adipocyte size in SC and VIS AT in both sexes (Fig. 2D). This may be attributed to alterations in lipid metabolism, increased oxidative stress and stiffening of the extracellular matrix (ECM), possibly indicating an induction of AT hypertrophy, as hypothesized previously (Schaffert et al., 2022). The reduced weight loss and adipocyte size after the recovery phase in male animals (Fig. 1C and 2E) may be attributed to increased hyperplasia and the development of new adipocytes from progenitors, thereby collectively maintaining the fat mass. In male animals, a potential shift may occur from hypertrophy (enlargement of existing adipocytes) to hyperplasia during the recovery period following dietary DINCH exposure. This process involves the differentiation of preadipocytes into mature adipocytes, driven by transcription factors such as PPARγ and C/EBP (Lehrke & Lazar, 2005; Rosen et al., 2002; Wu et al., 1999). It is typically assumed that the recruitment of adipose precursor cells primarily occurs during adolescence in humans (Spalding et al., 2008) and mice (Kim et al., 2014), and could thus be disturbed by chronic DINCH exposure. Further analyses, such as adipocyte size distribution using osmium-teroxide (Pietka & Abumrad, 2023), would provide a more comprehensive and reliable understanding of adipocyte number and adipocyte size distribution per gram of adipose tissue to confirm the proposed theory.

The administration of DINCH resulted in altered insulin sensitivity, as measured by an intraperitoneal insulin tolerance test, in female C57BL/6 mice (Fig. 4A). Similarly, the precursor plasticizer DEHP was observed to alter insulin tolerance in female 129S6 mice but not in males (Klöting et al., 2015). After the recovery period, during which mice were switched to a standard diet without DINCH, insulin sensitivity improved. Interestingly, DINCH exposed female mice showed a better recovery in insulin sensitivity compared to the HFD control group. Although the underlying mechanism is not yet understood, this observation suggests potential sex-specific effects that warrant further investigation. Additional measurements of insulin and C-peptide levels (Fig. 5A and B) and the insulin/C-peptide ratio (Fig. 5C) demonstrated a significant increase in male mice treated with the HD diet. Insulin and C-peptide are secreted from beta cells (β cells) in an equimolar ratio (Chen et al., 2023). In contrast to insulin, the liver does not extract C–peptide (Masharani & German, 2011). During the initial passage through the liver, up to 90 % of the secreted insulin is metabolized, while approximately 80 % of C-peptide is eliminated through the kidneys (Bonser et al., 1984; Zavaroni et al., 1987).The pre-existing insulin resistance in the HFD control group of male mice precluded the determination of any effect of DINCH (Fig. 4B). However, the significant increase in the insulin/C-peptide ratio between HD and HFD (Fig. 5C), suggests a possible increase in insulin resistance also in male mice.

In mature SGBS cells, exposure to 10 nM DINCH and MINCH significantly decreased adiponectin secretion while increasing leptin secretion (Schaffert et al., 2022). The serum adipokine levels in our *in vivo* model of diet-induced obesity did not show the same profiles (Fig. 5D and E). Despite the increase in adipocyte area, there was no significant change in body weight gain or in tissue weights of SC and VIS AT. This discrepancy may be attributed to the absence of the anticipated decrease in adiponectin and an increase in leptin levels, as observed *in vitro* (Schaffert et al., 2022).

The circulating lipid profiles exhibited a sexual dimorphism (Fig. 5F to I). The DINCH treatment resulted in elevated total cholesterol, HDL-, and LDL-cholesterol levels in male mice. In female mice, circulating triglycerides were elevated in the low DINCH group only (Fig. 5F). Exposure to DEHP has been linked to elevated levels of total serum cholesterol, non-HDL-cholesterol, and LDL-cholesterol in pregnant women (Mínguez-Alarcón et al., 2022). Conversely, metabolites of DINCH have been associated with reduced levels of serum HDL cholesterol (Mínguez-Alarcón et al., 2022). These findings contrast those of an earlier analysis, which did not find the effects of DINCH on rat serum cholesterol and triglycerides (Langsch et al., 2018). The robust correlation between lipoprotein modifications and insulin resistance underscores the potential metabolic hazards associated with DINCH exposure (Kannel, 1985; Manley, 1997).

Taken together, DINCH impacts insulin tolerance, as evidenced by alterations in the insulin/C-peptide ratio and ITT data (Fig. 4A/B and 5C). A notable disparity between the sexes was evident in all measurements. In light of these findings, further investigation into the sex-specific effects of DINCH on lipid metabolism and insulin resistance is warranted. This would be of particular interest also under SD baseline

conditions as hormonal and metabolic differences could influence its absorption and effects. We propose exploring these questions in future research to enhance our understanding of DINCH's impact across different dietary and physiological conditions.

In general, dietary DINCH exposure led to a relatively small proportion of proteins with significant changes in abundance in serum and the tissues analyzed (Fig. 7A and C). This is consistent with the concept of DINCH being a safe DEHP substitute with more favorable toxicological characteristics (Crespo et al., 2007; European Food Safety Authority (EFSA), 2006; Otter, 2016), even beyond concentrations achievable in everyday exposure scenarios. Yet, a *Reactome* pathway enrichment indicated alterations in processes associated with intermediary and central energy metabolism and immune response across all sample types analyzed (Fig. 7B). Given obesity as a metabolic disease characterized by dysfunctional adipose tissue and low-grade systemic inflammation (Valenzuela et al., 2023), this could indicate an amplification of these dysfunctionalities upon exposure to DINCH.

The liver, being the primary site of phase I drug metabolism by cytochrome P450 (CYP450) enzymes (Almazroo et al., 2017), shows an apparent response to the chemical burden by an enrichment of pathways related to the detoxification of xenobiotics in male mice (*xenobiotics, phase I functionalization of compounds, cytochrome P450 arranged by substrate type*; Fig. 7B). Interestingly, these pathways are not enriched in liver tissues from female mice (Fig. 7B). Still, selected CYP450s, including Cyp2c29, Cyp3a11, Cyp3a25 and Cyp2b10, were found at a significantly higher abundance in the treatment groups in male and female mice (Supplemental Fig. 19). While diet-induced obesity did not affect mRNA expression of Cyp2c29 and Cyp3a11 levels in C57BL/6 mice (Wang et al., 2020), in agreement with stable protein abundance in our data (HFD *vs* SD; Main Supplemental Files), the exposure towards xenobiotics commonly increases the expression of CYP enzymes through activation of nuclear receptors (NR) such as the aryl hydrocarbon receptor (AHR), constitutive androstane receptor (CAR) or pregnane-X-receptor (PXR) (Hakkola et al., 2018). Increased protein levels of Cyp2c29 and Cyp3a11 were shown following exposure to NR–activating azole fungicides in C57/B16 mice (Hammer et al., 2021) and in phenytoin-induced models of liver injury in C57BL/6 and C57BL/6J mice (Hagemeyer et al., 2010; Sasaki et al., 2013), implying that high–level DINCH exposure causes liver injury by a similar mechanism, possibly through NR mediated transcription/translation of Cyp2c/Cyp3a members.

Adipose tissue integrity of brown, visceral and subcutaneous depots indicated the enrichment of pathways associated with central metabolism (BAT, VIS and SC AT), translation (BAT) and cellular stress (VIS and SC AT) that were enhanced upon exposure to DINCH (Fig. 7B). This is in contrast to results from differentiated human subcutaneous SGBS adipocytes, which showed a decreased median abundance of central metabolic pathways at the protein level after exposure to mid-range concentrations of MINCH (μM) as the primary metabolite of DINCH for eight days (Schaffert et al., 2022). However, several studies demonstrated the potential of MINCH (μM) to induce adipogenesis in rat stromal vascular fraction (SVF) preadipocytes (Campioli et al., 2017), SGBS preadipocytes (Goerdeler et al., 2024; Schaffert et al., 2022) and 3 T3–L1 fibroblasts (Bereketoglu et al., 2024) at transcript, protein and metabolite level, thereby increasing the cells metabolic capacity. Besides differentiated adipocytes as the dominant cell type, the fraction of SVF cells is harbouring adipocyte progenitors, vascular and immune cells, among others, reflecting adipose tissue cell type heterogeneity (Maniyadath et al., 2023; Massier et al., 2023). Both findings could be covered in the results of this study, as a bulk proteome analysis of the whole tissue cannot distinguish between the different cell populations in adipose tissue, which means that cell type-specific responses to DINCH exposure are not recorded. Yet, the enrichment and increased abundance of central metabolic pathways upon dietary DINCH exposure might indicate a difference between *in vitro* and *in vivo* data, with its systemic connectivity and variety of cell types involved. In addition, the ability of pharmaceuticals and environmental chemicals to modulate NRs such as PPARγ can differ between model species (Garoche et al., 2021), potentially causing the observed discrepancies between studies.

Regulated and consistently significant candidates from the serum proteome analysis were primarily assigned to the immune system and adipose tissue secretory origins, indicating those as important sites of DINCH effective (Fig. 7D). In addition, VIS and SC AT of DINCH–exposed mice displayed a reduction in the interleukin–12 (IL-12) signalling pathway (Fig. 7B), highlighting immune responses to be involved during exposure. The reduction in tissue IL–12 signalling, as well as the decreased levels of interleukin–1 alpha (IL–1α) and C–C motif chemokine ligand 3 (Ccl3) in serum as pro-inflammatory cytokines and chemokine (Fig. 7B and C), suggest an altered systemic inflammatory state compared to HFD mice, potentially constructive for adipose tissue function (Valenzuela et al., 2023). In confirmation of the model, IL-1α was upregulated in the HFD– compared to SD–fed mice (significant in males; Main Supplemental File), as described for endogenous oils of human origin that were able to promote IL-1α release and foster the recruitment of M1–like macrophages and neutrophils (Tynan et al., 2014). Elsewhere, the knockout of IL-1α (Almog et al., 2019) and Ccl3 (Xu et al., 2021) in mice reduced their adiposity and steatohepatitis with hepatic fibrosis, respectively, while preventing HFD-induced adverse metabolic consequences. Conversely, the reduced levels could also be a compensatory mechanism to counteract prolonged or chronic inflammation. In apoptotic cells, IL-1α is retained chromatin-associated in the cell's nucleus without being released together with the cytoplasmic contents (Cohen et al., 2010). Consequently, this might impair the immune system's ability to react and defend itself and pave the way for infections or more severe metabolic disparities.

In male mice specifically, transforming growth factor-beta 1 (Tgf-β1) levels were reduced, while interleukin-17A (IL-17a) levels were elevated (Fig. 7C). This indicates a milieu of increased inflammatory activity and a potential shift towards a pro-inflammatory phenotype (Adamopoulos & Kuchroo, 2023; Biswas & Mantovani, 2010; Deng et al., 2024). Tgf-β1 is a dominantly immune cell-derived Tgf-β isoform and pleiotropic plasma cytokine (Prud'homme, 2007) that was identified to be integral for T-helper-17 (Th17) development (Mangan et al., 2006). While the reduced levels of Tgf-β1 reported here (Fig. 7C) do not necessarily support the observed increase in Th17 secreted IL–17a, a model of diet-induced obesity indicated the expression of *Acaca*, with its gene product acetyl-CoA carboxylase 1 (Acc1), to induce Th17 cell differentiation and increase IL-17a levels (Endo et al., 2015). This, in turn, goes well along the findings that metabolic pathways, including fatty acid metabolism in which Acc1 is decisively involved, were found positively enriched in adipose tissue of mice after dietary DINCH exposure (Fig. 7B), thereby enhancing the HFD-induced phenotypes. The increase in IL-17a following dietary DINCH exposure agrees with data on the endocrine disruptor bisphenol A (BPA), whose exposure correlated with IL-17a levels in human subjects with obesity. In addition, this relation was confirmed in a DIO mouse model of C57BL/6N mice that exhibited increased IL-17a levels after dietary BPA exposure (Hong et al., 2023). The effects specific to male mice possibly relate to the more pronounced establishment of the obesity mouse model in male compared to female mice (Fig. 1B and C).

In summary, the serum proteome revealed a complex picture of the inflammation and immune system-related changes induced by DINCH exposure, emphasizing the ability of DINCH to influence systemic processes.

5. Conclusion

Our study underscores the critical need to evaluate the physiological and functional impacts at the molecular level when assessing the metabolism-disrupting potential of chemicals. Concentration analysis of DINCH-exposed C57BL/6N mice confirmed that both DINCH and its metabolite, MINCH, were present in liver and adipose tissue, with

evidence suggesting possible bioaccumulation of DINCH in adipose tissue, as indicated by elevated levels following recovery. Phenotypic analysis revealed no significant increase in body weight, adipose tissue mass, or alterations in the distribution of lean and adipose tissue, consistent with existing approval studies that report no weight-promoting effects of DINCH treatment. However, detailed metabolic characterization revealed sex-specific effects: female mice exhibited reduced whole-body insulin sensitivity and elevated triglyceride levels, while male mice showed an altered insulin/C-peptide ratio and elevated cholesterol, HDL, and LDL levels. Proteomic profiling of serum and tissue proteins further identified alterations in pathways associated with central energy metabolism and immune responses, particularly highlighting changes in systemic inflammatory state induced by DINCH exposure. In conclusion, the observed sex-specific effects on insulin sensitivity, lipid metabolism, and inflammatory processes, along with potential bioaccumulation, should be considered in future risk assessments of DINCH and other potential metabolism-disrupting chemicals.

Funding

This work was supported by the *Deutsche Forschungsgemeinschaft* (DFG, German Research Foundation) through CRC 1052, project number *209933838*, subproject B1 to MB and MvB, and sub-project B4 to NK and sub-project Z3 to MvB. KS is grateful for funding from the *Deutsche Forschungsgemeinschaft* (DFG, German Research Foundation), project number *530364326*. KS: This work was carried out in the framework of the European Partnership for the Assessment of Risks from Chemicals (PARC) and has received funding from the European Union's Horizon Europe research and innovation programme under grant agreement no. 101057014. Views and opinions expressed are, however, those of the author(s) only and do not necessarily reflect those of the European Union or the Health and Digital Executive Agency. Neither the European Union nor the granting authority can be held responsible for them. KS, URK and MvB are grateful for funding of the UFZ for the ProMetheus platform for proteomics and metabolomics.

CRediT authorship contribution statement

Sontje Krupka: Writing – original draft, Visualization, Validation, Methodology, Investigation, Data curation, Conceptualization. **Alix Sarah Aldehoff:** Writing – original draft, Visualization, Validation, Methodology, Investigation, Data curation, Conceptualization. **Cornelius Goerdeler:** Writing – original draft, Visualization, Validation, Methodology, Investigation, Data curation, Conceptualization. **Beatrice Engelmann:** Writing – review & editing, Supervision, Methodology. **Ulrike Rolle-Kampczyk:** Writing – review & editing, Supervision, Conceptualization. **Kristin Schubert:** Writing – review & editing, Supervision, Investigation, Conceptualization. **Nora Klöting:** Writing – review & editing, Supervision, Conceptualization. **Martin von Bergen:** Writing – review & editing, Supervision, Project administration. **Matthias Blüher:** Writing – review & editing, Supervision, Project administration.

Declaration of competing interest

The authors declare that they have no known competing financial interests or personal relationships that could have appeared to influence the work reported in this paper.

Acknowledgement

The authors would like to express their gratitude to Jenny Schuster, Lisa Gärtner and Elisabeth Langer for their invaluable assistance in the care of the mice used in this study. Additionally, they would like to acknowledge the contributions of Susan Berthold, Anna Schaarschmidt and Melanie Börner in providing laboratory support and Kerstin Krause, Lisa Roth and Paul Czechowski for technical assistance with metabolic chambers and statistical advice. We thank Maj Schuster, Olivia Pleßow and Nicole Bock for their competent assistance with proteomic and metabolomic sample preparation and measurement. Figs. 1 and 6 were partly created with BioRender.

Appendix A. Supplementary data

Supplementary data to this article can be found online at https://doi.org/10.1016/j.envint.2025.109306.

Data availability

Proteomics data has been made available via PRIDE. Metabolomics data was uploaded to the Metabolomics Workbench. All other data will be made available upon request.

References

Adamopoulos, I. E., & Kuchroo, V. (2023). IL-17A and IL-17F in tissue homeostasis, inflammation and regeneration. Nature Reviews Rheumatology 2023 19:9, 19(9), 535-536. Doi: 10.1038/s41584-023-01004-5.

Almazroo, O.A., Miah, M.K., Venkataramanan, R., 2017. Drug Metabolism in the Liver. Clinics in Liver Disease 21 (1), 1–20. https://doi.org/10.1016/J.CLD.2016.08.001.

Almog, T., Kandel Kfir, M., Levkovich, H., Shlomai, G., Barshack, I., Stienstra, R., Lustig, Y., Leikin Frenkel, A., Harari, A., Bujanover, Y., Apte, R., Shaish, A., Harats, D., Kamari, Y., 2019. Interleukin-1α deficiency reduces adiposity, glucose intolerance and hepatic de-novo lipogenesis in diet-induced obese mice. BMJ Open Diabetes Research and Care 7 (1), e000650–e. https://doi.org/10.1136/BMJDRC-2019-000650.

Andrady, A.L., Neal, M.A., 2009. Applications and societal benefits of plastics. Philosophical Transactions of the Royal Society b: Biological Sciences 364 (1526), 1977–1984. https://doi.org/10.1098/RSTB.2008.0304.

Bates, D., Mächler, M., Bolker, B., Walker, S., 2015. Fitting Linear Mixed-Effects Models Using lme4. Journal of Statistical Software 67 (1), 1–48. https://doi.org/10.18637/jss.v067.i01.

Bereketoglu, C., Häggblom, I., Turanlı, B., Pradhan, A., 2024. Comparative analysis of diisononyl phthalate and di(isononyl)cyclohexane-1,2 dicarboxylate plasticizers in regulation of lipid metabolism in 3T3-L1 cells. Environmental Toxicology 39 (3), 1245–1257. https://doi.org/10.1002/TOX.24010.

Bhat, V.S., Durham, J.L., Ball, G.L., English, J.C., 2014. Derivation of an Oral Reference Dose (RfD) for the Nonphthalate Alternative Plasticizer 1,2-Cyclohexane Dicarboxylic Acid, Di-Isononyl Ester (DINCH). Journal of Toxicology and Environmental Health, Part B 17 (2), 63–94. https://doi.org/10.1080/10937404.2013.876288.

Biemann, R., Blüher, M., Isermann, B., 2021. Exposure to endocrine-disrupting compounds such as phthalates and bisphenol A is associated with an increased risk for obesity. Best Practice & Research Clinical Endocrinology & Metabolism 35 (5), 101546. https://doi.org/10.1016/J.BEEM.2021.101546.

Biswas, S. K., & Mantovani, A. (2010). Macrophage plasticity and interaction with lymphocyte subsets: cancer as a paradigm. Nature Immunology 2010 11:10, 11(10), 889-896. Doi: 10.1038/ni.1937.

Bonser, A.M., Garcia-Webb, P., Harrison, L.C., 1984. C-peptide measurement: methods and clinical utility. Critical Reviews in Clinical Laboratory Sciences 19 (4), 297–352. https://doi.org/10.3109/10408368409165766.

Borchers, H.W., 2023. pracma: Practical Numerical Math Functions. In.

Braeuning, A., Balaguer, P., Bourguet, W., Carreras-Puigvert, J., Feiertag, K., Kamstra, H. J., Knapen, D., Lichtenstein, D., Marx-Stoelting, P., Rietdijk, J., Schubert, K., Spjuth, O., Stinckens, E., Thedieck, K., Boom, D.V.R., Vergauwen, L., Bergen, V.M., Wewer, N., Zalko, D., 2023. Development of new approach methods for the identification and characterization of endocrine metabolic disruptors—a PARC project. Frontiers in Toxicology 5. https://doi.org/10.3389/ftox.2023.1212509.

Campioli, E., Lee, S., Lau, M., Marques, L., Papadopoulos, V., 2017. Effect of prenatal DINCH plasticizer exposure on rat offspring testicular function and metabolism. Scientific Reports 7 (1). https://doi.org/10.1038/s41598-017-11325-7.

Chen, J., Huang, Y., Liu, C., Chi, J., Wang, Y., Xu, L., 2023. The role of C-peptide in diabetes and its complications: an updated review. Frontiers in Endocrinology 14. https://doi.org/10.3389/FENDO.2023.1256093.

Cohen, I., Rider, P., Carmi, Y., Braiman, A., Dotan, S., White, M.R., Voronov, E., Martin, M.U., Dinarello, C.A., Apte, R.N., 2010. Differential release of chromatin-bound IL-1α discriminates between necrotic and apoptotic cell death by the ability to induce sterile inflammation. Proceedings of the National Academy of Sciences of the United States of America 107 (6), 2574–2579. https://doi.org/10.1073/PNAS.0915018107/SUPPL_FILE/PNAS.200915018SI.PDF.

Crespo, J.E., Balart, R., Sanchez, L., López, J., 2007. Substitution of di(2-ethylhexyl) phthalate by di(isononyl) cyclohexane-1,2-dicarboxylate as a plasticizer for industrial vinyl plastisol formulations. Journal of Applied Polymer Science 104 (2), 1215–1220. https://doi.org/10.1002/APP.25760.

Deng, Z., Fan, T., Xiao, C., Tian, H., Zheng, Y., Li, C., & He, J. (2024). TGF-β signaling in health, disease, and therapeutics. Signal Transduction and Targeted Therapy 2024 9: 1, 9(1), 1-40. Doi: 10.1038/s41392-024-01764-w.

Endo, Y., Asou, H.K., Matsugae, N., Hirahara, K., Shinoda, K., Tumes, D.J., Tokuyama, H., Yokote, K., Nakayama, T., 2015. Obesity Drives Th17 Cell Differentiation by Inducing the Lipid Metabolic Kinase, ACC1. Cell Reports 12 (6), 1042–1055. https://doi.org/10.1016/J.CELREP.2015.07.014.

9/815/EC: Commission Decision of 7 December 9 adopting measures prohibiting the placing on the market of toys and childcare articles intended to be placed in the mouth by children under three years of age made of soft PVC containing one or more of the substances di-iso-nonyl phthalate (DINP), di(2-ethylhexyl) phthalate (DEHP), dibutyl phthalate (DBP), di-iso-decyl phthalate (DIDP), di-n-octyl phthalate (DNOP), and butylbenzyl phthalate (BBP) (notified under document number C(9) 4436) (Text with EEA relevance), (9). https://eur-lex.europa.eu/eli/dec/9/815/oj.

European Food Safety Authority (EFSA). (2006). Opinion of the Scientific Panel on food additives, flavourings, processing aids and materials in contact with food (AFC) related to the 12th list of substances for food contact materials. EFSA Journal, 4(10), 395. Doi: 10.2903/J.EFSA.2006.395.

Ferrannini, E., 1988. The theoretical bases of indirect calorimetry: a review. Metabolism: Clinical and Experimental 37 (3), 287–301. https://doi.org/10.1016/0026-0495(88)90110-2.

FR-MSCA), A. o. b. (2016). Analysis of the most appropriate risk management option (RMOA).

Garoche, C., Boulahtouf, A., Grimaldi, M., Chiavarina, B., Toporova, L., Broeder, D.J.M., Legler, J., Bourguet, W., Balaguer, P., 2021. Interspecies Differences in Activation of Peroxisome Proliferator-Activated Receptor γ by Pharmaceutical and Environmental Chemicals. Environmental Science & Technology 55 (24), 16489–16501. https://doi.org/10.1021/acs.est.1c04318.

Giovanoulis, G., Bui, T., Xu, F., Papadopoulou, E., Padilla-Sanchez, A.J., Covaci, A., Haug, S.L., Cousins, P.A., Magnér, J., Cousins, T.I., Wit, D.A.C., 2018. Multi-pathway human exposure assessment of phthalate esters and DINCH. Environment International 112, 115–126. https://doi.org/10.1016/j.envint.2017.12.016.

Godwin, D. A. (2017). Plasticizers. In Applied Plastics Engineering Handbook (pp. 533-553).

Goerdeler, C., Engelmann, B., Aldehoff, A.S., Schaffert, A., Blüher, M., Heiker, J.T., Wabitsch, M., Schubert, K., Rolle-Kampczyk, U., von Bergen, M., 2024. Metabolomics in human SGBS cells as new approach method for studying adipogenic effects: Analysis of the effects of DINCH and MINCH on central carbon metabolism. Environmental Research 252, 118847. https://doi.org/10.1016/J.ENVRES.2024.118847.

Hagemeyer, C.E., Bürck, C., Schwab, R., Knoth, R., Meyer, R.P., 2010. 7-Benzyloxyresorufin-O-dealkylase activity as a marker for measuring cytochrome P450 CYP3A induction in mouse liver. Analytical Biochemistry 398 (1), 104–111. https://doi.org/10.1016/J.AB.2009.11.004.

Hakkola, J., Bernasconi, C., Coecke, S., Richert, L., Andersson, T.B., Pelkonen, O., 2018. Cytochrome P450 Induction and Xeno-Sensing Receptors Pregnane X Receptor, Constitutive Androstane Receptor, Aryl Hydrocarbon Receptor and Peroxisome Proliferator-Activated Receptor α at the Crossroads of Toxicokinetics and Toxicodynamics. Basic & Clinical Pharmacology & Toxicology 123, 42–50. https://doi.org/10.1111/BCPT.13004.

Hammer, H., Schmidt, F., Marx-Stoelting, P., Pötz, O., Braeuning, A., 2021. Cross-species analysis of hepatic cytochrome P450 and transport protein expression. Archives of Toxicology 95 (1), 117–133. https://doi.org/10.1007/S00204-020-02939-4/FIGURES/5.

Hao, C., Cheng, X., Xia, H., Ma, X., 2012. The endocrine disruptor mono-(2-ethylhexyl) phthalate promotes adipocyte differentiation and induces obesity in mice. Bioscience Reports 32 (6), 619–629. https://doi.org/10.1042/BSR20120042.

Harley, K. G., Berger, K., Rauch, S., Kogut, K., Claus Henn, B., Calafat, A. M., Huen, K., Eskenazi, B., & Holland, N. (2017). Association of prenatal urinary phthalate metabolite concentrations and childhood BMI and obesity. Pediatric Research 2017 82:3, 82(3), 405-415. Doi: 10.1038/pr.2017.112.

Harmon, P., Otter, R., 2022. A review of common non-ortho-phthalate plasticizers for use in food contact materials. Food and Chemical Toxicology 164, 112984. https://doi.org/10.1016/J.FCT.2022.112984.

Högberg, J., Hanberg, A., Berglund, M., Skerfving, S., Remberger, M., Calafat, M.A., Filipsson, F.A., Jansson, B., Johansson, N., Appelgren, M., Håkansson, H., 2008. Phthalate Diesters and Their Metabolites in Human Breast Milk, Blood or Serum, and Urine as Biomarkers of Exposure in Vulnerable Populations. Environmental Health Perspectives 116 (3), 334–339. https://doi.org/10.1289/ehp.10788.

Hong, X., Zhou, Y., Zhu, Z., Li, Y., Li, Z., Zhang, Y., Hu, X., Zhu, F., Wang, Y., Fang, M., Huang, Y., Shen, T., 2023. Environmental endocrine disruptor Bisphenol A induces metabolic derailment and obesity via upregulating IL-17A in adipocytes. Environment International 172, 107759. https://doi.org/10.1016/J.ENVINT.2023.107759.

Huang, T., Saxena, R.A., Isganaitis, E., James-Todd, T., 2014. Gender and racial/ethnic differences in the associations of urinary phthalate metabolites with markers of diabetes risk: national health and nutrition examination survey 2001–2008. Environmental Health 13 (1), 6. https://doi.org/10.1186/1476-069X-13-6.

Jéquier, E., 1989. Energy metabolism in human obesity. Sozial- Und Präventivmedizin SPM 34 (2), 58–62. https://doi.org/10.1007/BF02080082.

Kannel, W.B., 1985. Lipids, diabetes, and coronary heart disease: insights from the Framingham Study. American Heart Journal 110 (5), 1100–1107. https://doi.org/10.1016/0002-8703(85)90224-8.

Karkossa, I. (2023). proteomicsr: An analysis pipeline for label-based and label-free proteomics data. In: Zenodo.

Kasper-Sonnenberg, M., Koch, H.M., Apel, P., Rüther, M., Pälmke, C., Brüning, T., Kolossa-Gehring, M., 2019. Time trend of exposure to the phthalate plasticizer substitute DINCH in Germany from 1999 to 2017: Biomonitoring data on young adults from the Environmental Specimen Bank (ESB). International Journal of Hygiene and Environmental Health 222 (8), 1084–1092. https://doi.org/10.1016/J.IJHEH.2019.07.011.

Kim, M.S., Lun, M., Wang, M., Senyo, E.S., Guillermier, C., Patwari, P., Steinhauser, L.M., 2014. Loss of White Adipose Hyperplastic Potential Is Associated with Enhanced Susceptibility to Insulin Resistance. Cell Metabolism 20 (6), 1049–1058. https://doi.org/10.1016/j.cmet.2014.10.010.

Klöting, N., Hesselbarth, N., Gericke, M., Kunath, A., Biemann, R., Chakaroun, R., Kosacka, J., Kovacs, P., Kern, M., Stumvoll, M., Fischer, B., Rolle-Kampczyk, U., Feltens, R., Otto, W., Wissenbach, D.K., Von Bergen, M., Blüher, M., 2015. Di-(2-ethylhexyl)-phthalate (DEHP) causes impaired adipocyte function and alters serum metabolites. PLoS ONE 10 (12). https://doi.org/10.1371/journal.pone.0143190.

Klöting, N., Koch, L., Wunderlich, T., Kern, M., Ruschke, K., Krone, W., Brüning, J.C., Blüher, M., 2008. Autocrine IGF-1 Action in Adipocytes Controls Systemic IGF-1 Concentrations and Growth. Diabetes 57 (8), 2074–2082. https://doi.org/10.2337/db07-1538.

Koch, H.M., Schütze, A., Pälmke, C., Angerer, J., Brüning, T., 2013. Metabolism of the plasticizer and phthalate substitute diisononyl- cyclohexane-1,2-dicarboxylate (DINCH®) in humans after single oral doses. Archives of Toxicology 87 (5), 799–806. https://doi.org/10.1007/S00204-012-0990-4/TABLES/2.

Langsch, A., David, R. M., Schneider, S., Sperber, S., Haake, V., Kamp, H., Leibold, E., Ravenzwaay, B. v., & Otter, R. (2018). Hexamoll® DINCH: Lack of in vivo evidence for obesogenic properties. Toxicology Letters, 288, 99-110. Doi: 10.1016/j.toxlet.2018.02.008.

Lefterova, M.I., Haakonsson, A.K., Lazar, M.A., Mandrup, S., 2014. PPARγ and the global map of adipogenesis and beyond. Trends in Endocrinology & Metabolism 25 (6), 293–302. https://doi.org/10.1016/J.TEM.2014.04.001.

Lehrke, M., Lazar, A.M., 2005. The Many Faces of PPARγ. Cell 123 (6), 993–999. https://doi.org/10.1016/j.cell.2005.11.026.

Little, T. A. (2015). Method Validation Essentials, Limit of Blank, Limit of Detection, and Limit of Quantitation. BioPharm International, 28(4), 48-51. https://www.biopharminternational.com/view/method-validation-essentials-limit-blank-limit-detection-and-limit-quantitation.

Mangan, P. R., Harrington, L. E., O'Quinn, D. B., Helms, W. S., Bullard, D. C., Elson, C. O., Hatton, R. D., Wahl, S. M., Schoeb, T. R., & Weaver, C. T. (2006). Transforming growth factor-β induces development of the TH17 lineage. Nature 2006 441:7090, 441(7090), 231-234. Doi: 10.1038/nature04754.

Maniyadath, B., Zhang, Q., Gupta, R.K., Mandrup, S., 2023. Adipose tissue at single-cell resolution. Cell Metabolism 35 (3), 386–413. https://doi.org/10.1016/J.CMET.2023.02.002.

Manley, S.E., 1997. U.K. Prospective Diabetes Study 27: Plasma lipids and lipoproteins at diagnosis of NIDDM by age and sex. Diabetes Care 20 (11), 1683–1687. https://doi.org/10.2337/DIACARE.20.11.1683.

Maric, I., Krieger, J.P., van der Velden, P., Börchers, S., Asker, M., Vujicic, M., Wernstedt Asterholm, I., Skibicka, K.P., 2022. Sex and Species Differences in the Development of Diet-Induced Obesity and Metabolic Disturbances in Rodents. Frontiers in Nutrition 9. https://doi.org/10.3389/FNUT.2022.828522/FULL.

Masharani, U., & German, M. S. (2011). Pancreatic Hormones and Diabetes Mellitus. In 9 (Ed.), Greenspan's Basic & Clinical Endocrinology. https://accessmedicine.mhmedical.com/content.aspx?bookid=380&sectionid=39744057.

Massier, L., Jalkanen, J., Elmastas, M., Zhong, J., Wang, T., Nono Nankam, P. A., Frendo-Cumbo, S., Bäckdahl, J., Subramanian, N., Sekine, T., Kerr, A. G., Tseng, B. T. P., Laurencikiene, J., Buggert, M., Lourda, M., Kublickiene, K., Bhalla, N., Andersson, A., Valsesia, A., . . . Mejhert, N. (2023). An integrated single cell and spatial transcriptomic map of human white adipose tissue. Nature Communications 2023 14:1, 14(1), 1-19. Doi: 10.1038/s41467-023-36983-2.

McNally, K., Sams, C., Loizou, G., 2019. Development, Testing, Parameterization, and Calibration of a Human Physiologically Based Pharmacokinetic Model for the Plasticizer, Hexamoll® Diisononyl-Cyclohexane-1, 2-Dicarboxylate Using In Silico, In Vitro, and Human Biomonitoring Data. Frontiers in Pharmacology 10, 1394. https://doi.org/10.3389/fphar.2019.01394.

Meeker, J.D., Sathyanarayana, S., Swan, S.H., 2009. Phthalates and other additives in plastics: human exposure and associated health outcomes. Philosophical Transactions of the Royal Society b: Biological Sciences 364 (1526), 2097–2113. https://doi.org/10.1098/RSTB.2008.0268.

Milacic, M., Beavers, D., Conley, P., Gong, C., Gillespie, M., Griss, J., Haw, R., Jassal, B., Matthews, L., May, B., Petryszak, R., Ragueneau, E., Rothfels, K., Sevilla, C., Shamovsky, V., Stephan, R., Tiwari, K., Varusai, T., Weiser, J., D'Eustachio, P., 2024. The Reactome Pathway Knowledgebase 2024. Nucleic Acids Research 52 (D1), D672–D678. https://doi.org/10.1093/nar/gkad1025.

Mínguez-Alarcón, L., Williams, P.L., James-Todd, T., Souter, I., Ford, J.B., Rexrode, K.M., Calafat, A.M., Hauser, R., Chavarro, J.E., 2022. Association of Urinary Phthalate and Phthalate Replacement Metabolite Concentrations with Serum Lipid Biomarker Levels among Pregnant Women Attending a Fertility Center. Toxics 10 (6). https://doi.org/10.3390/TOXICS10060292/S1.

Müller, M.J., Enderle, J., Bosy-Westphal, A., 2016. Changes in Energy Expenditure with Weight Gain and Weight Loss in Humans. Current Obesity Reports. https://doi.org/10.1007/s13679-016-0237-4.

Risk Factor Collaboration. (2017). Worldwide trends in body-mass index, underweight, overweight, and obesity from 1975 to 2016: a pooled analysis of 2416 population-based measurement studies in 128·9 million children, adolescents, and adults. The Lancet, 390(10113), 2627-2642. Doi: 10.1016/S0140-6736(17)32129-3.

Otter, R., 2016. The publication "Cyclohexane-1,2-dicarboxylic acid diisononyl ester and metabolite effects on rat epididymal stromal vascular fraction differentiation of adipose tissue" by Enrico Campioli, Tam B. Duong, François Deschamps, Vassilios Papadopoulos, Environmental Research 140 (2015), 145–156, merits some critical comments. Environmental Research 144, 165–166. https://doi.org/10.1016/J.ENVRES.2015.08.021.

Perez-Riverol, Y., Csordas, A., Bai, J., Bernal-Llinares, M., Hewapathirana, S., Kundu, D. J., Inuganti, A., Griss, J., Mayer, G., Eisenacher, M., Pérez, E., Uszkoreit, J., Pfeuffer, J., Sachsenberg, T., Yilmaz, Ş., Tiwary, S., Cox, J., Audain, E., Walzer, M., Vizcaíno, J.A., 2019. The PRIDE database and related tools and resources in 2019: improving support for quantification data. Nucleic Acids Research 47 (D1), D442–D450. https://doi.org/10.1093/NAR/GKY1106.

Pietka, T.A., Abumrad, N.A., 2023. Determination of Adipocyte Size and Number. Thermogenic Fat. https://doi.org/10.1007/978-1-0716-3167-6_4.

Prud'homme, G.J., 2007. Pathobiology of transforming growth factor β in cancer, fibrosis and immunologic disease, and therapeutic considerations. Laboratory Investigation 87 (11), 1077–1091. https://doi.org/10.1038/LABINVEST.3700669.

R Core Team. (2023). R: A Language and Environment for Statistical Computing. In. Vienna, Austria.

Rosen, D.E., Hsu, C.-H., Wang, X., Sakai, S., Freeman, W.M., Gonzalez, J.F., Spiegelman, M.B., 2002. C/EBPα induces adipogenesis through PPARγ: a unified pathway. Genes & Development 16 (1), 22–26. https://doi.org/10.1101/gad.948702.

Sasaki, E., Matsuo, K., Iida, A., Tsuneyama, K., Fukami, T., Nakajima, M., Yokoi, T., 2013. A Novel Mouse Model for Phenytoin-Induced Liver Injury: Involvement of Immune-Related Factors and P450-Mediated Metabolism. Toxicological Sciences 136 (1), 250–263. https://doi.org/10.1093/TOXSCI/KFT184.

Schaffert, A., Arnold, J., Karkossa, I., Blüher, M., von Bergen, M., Schubert, K., 2021. The Emerging Plasticizer Alternative DINCH and Its Metabolite MINCH Induce Oxidative Stress and Enhance Inflammatory Responses in Human THP-1 Macrophages. Cells 10 (9), 2367. https://doi.org/10.3390/cells10092367.

Schaffert, A., Karkossa, I., Ueberham, E., Schlichting, R., Walter, K., Arnold, J., Blüher, M., Heiker, J.T., Lehmann, J., Wabitsch, M., Escher, B.I., von Bergen, M., Schubert, K., 2022. Di-(2-ethylhexyl) phthalate substitutes accelerate human adipogenesis through PPARγ activation and cause oxidative stress and impaired metabolic homeostasis in mature adipocytes. Environment International 164, 107279. https://doi.org/10.1016/J.ENVINT.2022.107279.

Schmidt, J.S., Schaedlich, K., Fiandanese, N., Pocar, P., Fischer, B., 2012. Effects of Di(2-ethylhexyl) phthalate (DEHP) on female fertility and adipogenesis in C3H/N Mice. Environmental Health Perspectives 120 (8), 1123–1129. https://doi.org/10.1289/EHP.1104016/ASSET/F3FDAB7D-08D7-40C8-BE97-7E94BD728A9F/ASSETS/GRAPHIC/EHP.1104016.G005.JPG.

Schütze, A., Pälmke, C., Angerer, J., Weiss, T., Brüning, T., Koch, M.H., 2012. Quantification of biomarkers of environmental exposure to di(isononyl)cyclohexane-1,2-dicarboxylate (DINCH) in urine via HPLC–MS/MS. Journal of Chromatography B 895–896, 123–130. https://doi.org/10.1016/j.jchromb.2012.03.030.

Spalding, L.K., Arner, E., Westermark, O.P., Bernard, S., Buchholz, A.B., Bergmann, O., Blomqvist, L., Hoffstedt, J., Näslund, E., Britton, T., Concha, H., Hassan, M., Rydén, M., Frisén, J., Arner, P., 2008. Dynamics of fat cell turnover in humans. Nature 453 (7196), 783–787. https://doi.org/10.1038/nature06902.

Speakman, J.R., 2013. Measuring Energy Metabolism in the Mouse – Theoretical, Practical, and Analytical Considerations. Frontiers in Physiology 4. https://doi.org/10.3389/fphys.2013.00034.

Specht, O.I., Toft, G., Hougaard, S.K., Lindh, H.C., Lenters, V., Jönsson, A.G.B., Heederik, D., Giwercman, A., Bonde, E.P.J., 2014. Associations between serum phthalates and biomarkers of reproductive function in 589 adult men. Environment International 66, 146–156. https://doi.org/10.1016/j.envint.2014.02.002.

Staskal, D.F., Diliberto, J.J., Birnbaum, L.S., 2006. Impact of Repeated Exposure on the Toxicokinetics of BDE 47 in Mice. Toxicological Sciences 89 (2), 380–385. https://doi.org/10.1093/TOXSCI/KFJ038.

Stevens, S., Bartosova, Z., Völker, J., Wagner, M., 2024. Migration of endocrine and metabolism disrupting chemicals from plastic food packaging. Environment International 189, 108791. https://doi.org/10.1016/j.envint.2024.108791.

Tynan, G.A., Hearnden, C.H., Oleszycka, E., Lyons, C.L., Coutts, G., O'Connell, J., Corrigan, M.A., Lynch, L., Campbell, M., Callanan, J.J., Mok, K.H., Geoghegan, J., O'Farrelly, C., Allan, S.M., Roche, H.M., O'Shea, D.B., Lavelle, E.C., 2014. Endogenous Oils Derived From Human Adipocytes Are Potent Adjuvants That Promote IL-1α–Dependent Inflammation. Diabetes 63 (6), 2037–2050. https://doi.org/10.2337/DB13-1476.

Useini, A., Engelberger, F., Künze, G., Sträter, N., 2023. Structural basis of the activation of PPARγ by the plasticizer metabolites MEHP and MINCH. Environment International 173, 107822. https://doi.org/10.1016/j.envint.2023.107822.

Valenzuela, P. L., Carrera-Bastos, P., Castillo-García, A., Lieberman, D. E., Santos-Lozano, A., & Lucia, A. (2023). Obesity and the risk of cardiometabolic diseases. Nature Reviews Cardiology 2023 20:7, 20(7), 475-494. Doi: 10.1038/s41569-023-00847-5.

Wang, P., Shao, X., Bao, Y., Zhu, J., Chen, L., Zhang, L., Ma, X., Zhong, X., 2020. Impact of obese levels on the hepatic expression of nuclear receptors and drug-metabolizing enzymes in adult and offspring mice. Acta Pharmaceutica Sinica B 10 (1), 171–185. https://doi.org/10.1016/J.APSB.2019.10.009.

Wright, S.L., Kelly, F.J., 2017. Plastic and Human Health: A Micro Issue? Environmental Science and Technology 51 (12), 6634–6647. https://doi.org/10.1021/ACS.EST.7B00423/SUPPL_FILE/ES7B00423_SI_001.PDF.

Wu, Z., Rosen, D.E., Brun, R., Hauser, S., Adelmant, G., Troy, E.A., Mckeon, C., Darlington, J.G., Spiegelman, M.B., 1999. Cross-Regulation of C/EBPα and PPARγ Controls the Transcriptional Pathway of Adipogenesis and Insulin Sensitivity. Molecular Cell 3 (2), 151–158. https://doi.org/10.1016/S1097-2765(00)80306-8.

Xu, L., Chen, Y., Nagashimada, M., Ni, Y., Zhuge, F., Chen, G., Li, H., Pan, T., Yamashita, T., Mukaida, N., Kaneko, S., Ota, T., Nagata, N., 2021. CC chemokine ligand 3 deficiency ameliorates diet-induced steatohepatitis by regulating liver macrophage recruitment and M1/M2 status in mice. Metabolism 125, 154914. https://doi.org/10.1016/J.METABOL.2021.154914.

Yaghjyan, L., Sites, S., Ruan, Y., & Chang, S. H. (2015). Associations of urinary phthalates with body mass index, waist circumference and serum lipids among females: National Health and Nutrition Examination Survey 1999–2004. International Journal of Obesity 2015 39:6, 39(6), 994-1000. Doi: 10.1038/ijo.2015.8.

Yang, Y., Smith, D.L., Keating, K.D., Allison, D.B., Nagy, T.R., 2014. Variations in body weight, food intake and body composition after long-term high-fat diet feeding in C57BL/6J Mice. Obesity (Silver Spring. Md.) 22 (10), 2147. https://doi.org/10.1002/OBY.20811.

Zavaroni, I., Deferrari, G., Lugari, R., Bonora, E., Garibotto, G., Dall'aglio, E., Robaudo, C., & Gnudi, A. (1987). Renal metabolism of C-peptide in man. The Journal of clinical endocrinology and metabolism, 65(3), 494-498. Doi: 10.1210/JCEM-65-3-494.